Utah Chapter EERI Short Course

Evaluation and Mitigation of Liquefaction Hazard for Engineering Practice

Wednesday April 9th, 2014

Maverik Center, West Valley, Utah

W.D. Liam Finn, University of British Columbia, Vancouver, Canada

Invited Instructor

This lecture material is an updating and extension of guidelines originally developed for the British Columbia Schools Seismic Retrofit Program by

W.D. Liam Finn and Jason Dowling, University of British Columbia

A. Wightman, BGC Engineering, Vancouver

John Sherstobitoff, Ausenco Ltd, Vancouver

Table of Contents

Executive Summary

Guidelines for Evaluating Liquefaction Potential and Consequences

These guidelines provide state of the art information and guidance on

- Site Investigation
- Evaluation of Liquefaction Potential
- Consequences of Liquefaction in terms of Ground Displacements
- Mitigation of Liquefaction effects by structural retrofits and geotechnical measures

Introduction

The 1964 earthquakes in Niigata and Alaska caused devastating damage to structures and all kinds of infrastructure as a result of widespread liquefaction. Reconstruction required a good understanding of the mechanics of liquefaction but little was known about liquefaction at the time. Major research programs were initiated by the Universities of California and Tokyo to support safe reconstruction and both made significant and lasting contributions to the evaluation of the potential for the triggering of liquefaction and quantifying the effects of liquefaction in terms of lateral spreading, settlement and slope failures.

In the beginning the study of liquefaction was based on cyclic loading tests of reconstituted samples. These tests were very useful for defining the mechanics of liquefaction and giving insight into potential consequences but it was quickly realized that such samples were not representative of field conditions and therefore could not be relied upon to assess the liquefaction potential in the field. Attention turned to the possibility of using in situ penetration tests to assess the density and hence the resistance of soils in situ to liquefaction. These studies have resulted in the development of Liquefaction Assessment Charts based on SPT-N, CPT-q_c and for soils that are difficult to penetrate, charts based on shear wave velocity, Vs. In the early days, site response analysis was not a viable option, so Seed and Idriss (1971) developed a simplified method for estimating the cycles of uniform stress representative of the actual shaking intensity of the earthquake. This approach, despite advances in computational capacity, is still very widely used.

The approach described above is a deterministic approach based on a specified design earthquake and an associated peak ground acceleration. At present a number of codes specify site hazard probabilistically, mostly a hazard with an exceedance rate of 2% in 50 years. To deal with probabilistic ground motions, the approach to evaluating liquefaction hazard using the simplified method requires some modifications.

These course notes describe both the deterministic and probabilistic approaches to the evaluation of liquefaction potential and its consequences. The simplified method was developed for sands and cohesionless silts. It has become clear, especially from field data from recent Turkish earthquakes that fine grained plastic soils can also suffer strength loss and stiffness degradation under cyclic loading. The course notes describe how these soils can be evaluated in the simplified framework when necessary modifications are made.

Finally the course notes review remediation options and stress the importance of evaluating the potential of either structural or geotechnical retrofits. Cases where structural retrofits are cheaper are not uncommon for smaller buildings. The course ends with a “Closing the Loop” example, showing the value of informed interaction between Structural and Geotechnical Engineers.

1.0 Site Investigation

1.1 Geology

Desk studies should include reference to surficial geological maps and reports, supplemented by air photo interpretation and ground truthing where appropriate. Liquefaction hazard maps are also useful sources of information. The aim should be to identify areas underlain by normally consolidated deposits of Pleistocene and Holocene age, as well as regions of flooding and/or high ground water levels. It is important to identify any areas of filled ground, especially in coastal or riverine environments where loose fills might extend below the water line.

1.2 Geotechnical Site Investigation Techniques

The resistance of soil deposits to liquefaction is usually determined using in-situ testing comprising one or more of penetration tests, such as the Standard Penetration Test (SPT) or the Cone Penetration Test (CPT), or measurement of shear wave velocity, V_s. The CPT may include measurement of pore-water pressure, u, (CPTu) or seismic shear wave velocity, V_s. For the case of soft silty clays and low plastic silts, although these types of soils may not liquefy in the traditional sense, earthquake shaking can often exceed cyclic strength and produce significant cyclic softening and deformation response. This is often best evaluated using undisturbed sampling and laboratory testing supported by in-situ vane shear testing and/or CPTu.

(1) Standard Penetration Testing

The original work to characterize liquefaction resistance was correlated to the Standard Penetration Test (SPT). In more recent years the Cone Penetration Test (CPT) has come into favor because of its greater level of standardization and repeatability, given suitable soils free of gravels and cemented layers. The SPT may often still be the method of choice, especially when the recovery of samples for laboratory index testing forms an important part of the evaluation. However push samples can now be retrieved by the CPT. When using SPT to characterize liquefaction resistance it is important that the testing be carried out according to ASTM D-606 to ensure repeatable, reliable results. Some of the standard features of reliable SPT testing are listed below, starting with the drilling of the test hole.

- Test holes should be drilled using techniques that minimize disturbance of the bottom of the hole prior to sampling. When drilling below the water table, this usually requires using rotary drilling with mud as a drilling fluid to stabilize the walls and base of the hole. The drill bit used should not jet drilling fluid vertically downwards as this would disturb the base of the hole. A modified tricone bit that jets laterally or upwards is the preferred method. Under no circumstances should air-flush, hollow stem augers, or vibratory drilling methods be used when reliable SPT measurements are required
- In order to be sure that SPT sampling is being carried out in undisturbed soil beyond the base of the hole, it is good practice for the supervising engineer to record the depth drilled prior to sampling and also to record and compare this with the depth to

the tip of the split spoon sampler, to ensure that there has been no caving or heaving of the base of the hole. Collapse of the base of the hole can be a problem especially in loose fine sands. Adopting as standard practice the slow withdrawal of the drill string, while at the same time maintaining a head of drill mud in the hole at the ground level or top of the mud pan, will usually solve heave and caving at the base of the hole.

  - The SPT test procedure should include a record of the type of hammer used, i.e automatic or manual drop, style of hammer (donut or safety), number of wraps on the cathead, if manual, dimensions of the sampling rod string (Aw, HW, Bw etc.), and the details of the split spoon. In the latter case it is important for the supervising engineer to record whether or not the split spoon is designed to accommodate a split liner, and if so whether or not a liner is being used. All drill rod joints should be wrenched tight.
  - SPT test has the ability to recover a soil sample for inspection and testing. This is often problematic in loose fine sands, however. Sample recovery can be improved by making sure that the split spoon head assembly contains a fully functioning ball valve, with vent holes above, to seal off the sample from any out of balance pressure from dill mud within the rod string as the sampler is withdrawn from the test hole. The use of a plastic sand catcher in the tip of the spoon, augmented with a loose wrap of cling film on its upper surface, is also recommended to enhance sample recovery in loose ground.

- One of the most important variables in SPT testing is the amount of energy delivered to the drill string by the falling hammer. Research in the mid-1980s determined that the average North American SPT procedures resulted in energy input to the rod string below the hammer anvil amounted to 60% of theoretical maximum potential energy of a 140 Lb. hammer falling 30 inches. Some regional and national variations were determined, and the profession adopted a “Standard” rod energy ratio of 60% for correlation of liquefaction field performance and standardization of data from different drill rigs and hammer assemblies. The routine use of instrumentation to measure the energy delivered to the SPT rod string, at sites with liquefaction potential, is strongly recommended in preference to the use of generic correction factors such as those given by Seed et al. (1985). The equipment and expertise needed to carry out such tests during drilling and sampling are now available.
- The SPT test is most reliable when used in sands and silty sands, but on occasion is used to estimate the liquefaction resistance of gravelly soils. When this is the case the recording of incremental 1” blow counts is recommended. The blows are counted for each 1” of penetration, rather than in 6” increments used for standard testing. Comparing the variability within the typical 12 to 18 such values, usually by plotting cumulative penetration versus blow count and noting changes in slope, can enable the engineer to estimate where the penetration resistance has been influenced by the coarse fraction of the sample interfering with the sampler. A more reliable blow count, more representative of only the sand fraction can usually be estimated from such data sets, by extrapolating a short interval measurement to an equivalent 12-inch penetration resistance. This technique is usually most applicable to soils with at least 50% passing the No. 4 sieve.

Additional guidance is given by Andrus and Youd (1987), and Vallee and Skryness (1980).

(2) Cone Penetration Testing

There are several reputable cone contractors available and the industry can now be considered mature and reliable. The advantage of using CPT equipment for liquefaction assessments is that it provides a continuous profile with depth, and so is less likely to miss thin layers of loose or fine grained materials which can have major influence on liquefaction and post-liquefaction performance. Another advantage of the CPT method is its repeatability and standardization. But even so there are things to which the supervising engineer should pay close attention. The size and type of CPT tip should be noted and recorded. There are two different sizes in common use, a 10 sq.cm tip and a 15 sq.cm tip. The capacity and sensitivity of the cone tip should be selected with care so as not to use too high a capacity cone in very soft soils and vice-versa. The location of the pore pressure sensor and attention to the details of its saturation are very important. In cases where the water table is not close to the ground surface the pore pressure sensor can become de-saturated on the initial push. Sometimes it is an advantage to make the cone push in two stages, the first one without a pore pressure tip, or with a blank tip, to ream out the hole and allow rapid deployment of a fully saturated tip down to the water table.

A disadvantage of CPT is the lack of a soil sample and the uncertainty associated with soil classification and particularly with the determination of fines content. Several soil type interpretation correlations with CPT have been developed in recent years and there is still ongoing research on this topic. Some of the more recent versions of CPT interpretation methods are discussed in Robertson (2010). It is recommended that reliance not be placed totally on such techniques, especially for estimating fines content, so that any CPT investigation program should be accompanied by a minimum of one sampled boring with good sample recovery that enables laboratory testing for grain size, fines content, water content and plasticity. Push samples can be recovered near the CPT location using the cone to push the samples. Experience has shown that the correlation of fines content with the cone parameter, I_c, is problematic. Even site-specific correlations, developed using side by side SPT borings and CPT, cannot always be used with confidence at other locations on the same site with ostensibly similar geology.

(3) Shear Wave Velocity Measurements

The ability of a soil to transmit shear waves is related to density and effective confining stress. Shear wave velocity determined in-situ with geophysical techniques is a small strain parameter that might be related to the small threshold strains which are needed to trigger liquefaction (Dobry and Abdoun 2011). There is therefore a correlation between shear wave velocity and liquefaction triggering stresses, but it tends to be somewhat subdued in comparison to CPT and SPT based correlations. The most common methods for determination of shear wave velocity are down-hole, cross-hole, and non-invasive surface methods such as shear wave refraction, SASW, and MASW. The seismic CPT is a variant of the down-hole method. There are also up-hole techniques that are derived from oil well logging technology which tend to be expensive and are used more for very deep holes.

(4) V_s from Ambient Motions

An innovative new method, based on ambient vibration measurements, has been developed for determining the shear wave velocity profile of a site to provide a more economic approach to Site Class Identification by V_{s30}. The recorded motions are inverted using a Monte Caro technique to give the best estimate of the velocity profile. The efficacy of this derived S in evaluating liquefaction potential will be illustrated later.

(5) Undisturbed Sampling

The evaluation of the earthquake behavior of saturated clays and plastic silts requires an understanding of undrained strength and in-situ states of stress and stress history (Idriss and Boulanger, 2008). It is often necessary to obtain high quality undisturbed samples for laboratory testing. Undisturbed sampling of clayey silts and silty clays for laboratory testing is best done using thin-walled tubes and a fixed piston sampler. A discussion of the factors involved in sampling and testing of fine grained soils for purposes of determining shear strength and earthquake resistance is given in the works of Ladd and DeGroot (2003), DeGroot and Ladd (2012), and Idriss and Boulanger (2008).

(6) In-Situ Shear Strengths of Fine-Grained Soils

To aid in the determination of undrained strength and stress history (OCR) it is common to determine undrained strength by in-situ methods. Although there are empirical correlations of undrained strength with CPT cone tip resistance, q_t, the range of uncertainty is significant, with cone factor N_{kt} varying typically between 10 and 18. A preferred in-situ testing procedure is to use a downhole vane with controlled rate of loading at the surface, such as a Nilcon vane borer or an electric down-hole vane. High quality measurements of undrained strength obtained in this manner can be used to develop site-specific cone calibrations if necessary on larger projects.

1.3 Scope of investigations

The extent of site investigations needed to establish the likely performance of school buildings in potentially liquefiable ground may vary considerably from site to site, to the degree that no one scope of work fits all cases. Things to consider are the layout of school buildings in plan, the presence of any sloping ground or deep open ditches and drainage canals, or river banks. In general a phased approach to site investigations is recommended, with a minimum of three test locations spaced strategically around the facilities as the first stage. If significant liquefaction issues are identified, and ground conditions are not uniform, then additional investigation may be appropriate. The structural engineer assessing school retrofit requirements is usually interested in knowing the potential for differential movements, both vertically and horizontally. Assessment of this is influenced by the depth, variability and continuity of potentially liquefiable materials, as well as the types of foundations at the school. Often a suitable strategy in the Fraser Delta area, in the absence of prior information, is to use the first test hole to explore to a depth of about 30 m, or at least 5 m of penetration into non-liquefiable soils, and then select the depth of subsequent test holes to identify variability and continuity of problematic zones across the site. The first test hole or CPTu can be used to determine a shear wave velocity profile for subsequent use in one or more of site classification, site response modeling, and liquefaction triggering assessments.

A good example of how knowledge of spatial heterogeneity can affect an assessment of liquefaction performance of a building is given in Idriss and Boulanger (2008), Chapter 4.

2.0 Evaluation of Liquefaction Potential

2.1 Introduction

Guidelines are presented for assessing the potential for triggering liquefaction and for estimating post-liquefaction lateral spreading displacements and settlements. Unfortunately these are transitional guidelines because an US NRC committee entitled the *National Research Council Committee on State of the Art and Practice in Earthquake Induced Liquefaction Assessment* will start work to investigate the current status of research and practice for assessing liquefaction potential and to formulate a generally acceptable state of practice. It is hoped that their report will resolve the controversy over the relative merits of the Idriss and Boulanger (2008) and the Cetin et al. (2004) approaches for evaluating liquefaction potential that has troubled the profession over the last few years.

The generally accepted state of practice for assessing the potential for triggering liquefaction is set out in Youd et al. (2001). EERI published a monograph by Idriss and Boulanger in 2008 entitled *"Soil Liquefaction during Earthquakes"* which conducted a global review of research and practice up to 2007 and made new recommendations for evaluating the triggering of liquefaction. In these tentative guidelines, the Youd et al. (2001) and the Idriss and Boulanger (2008) procedures are presented in parallel. This selection is based on the assumption that eventually Idriss and Boulanger (2008) will be substantially adopted as good practice.

2.2 Simplified method for seismic stress analysis

The simplified approach estimates average cyclic shear stress ratios (CSR) caused by earthquake shaking using **Equation 1,**

$$CSR = 0.65\frac{a_{max}}{g}\cdot\frac{\sigma_{v0}}{\sigma'_{v0}}\cdot\frac{r_d}{MSF} \qquad (\mathbf{1})$$

where a_{max} = peak ground surface acceleration, g = acceleration of gravity (in same units as a_{max}), σ_{vo} and σ'_{vo} = total and effective vertical stresses at the depth of interest, and r_d = depth reduction factor, and MSF is a magnitude scaling factor factor which weights the contribution of each magnitude to liquefaction potential relative to the reference magnitude M=7.5. For M=7.5, MSF=1.0. The MSF according to Youd et al. (2001) and Idriss and Boulanger (2008) are given in **Table 1**.

Table 1. Magnitude Scaling Factors, MSF

NCEER Youd et al. (2001)	Idriss and Boulanger (2008)
$MSF = \dfrac{10^{2.24}}{M_w^{\ 2.56}}$	$MSF = \min \text{ of } \left[6.9\exp\left(\dfrac{-M_w}{4}\right) - 0.058\right]$ or 1.8

The two sets of factors are plotted as a function of magnitude in **Figure 1**. There is significant difference between the two sets of MSF. Other things being equal, the Idriss and Boulanger (2008) MSF will lead to much larger Cyclic Stress Ratios, (CSR), for smaller earthquake magnitudes than Youd et al. (2001) does..

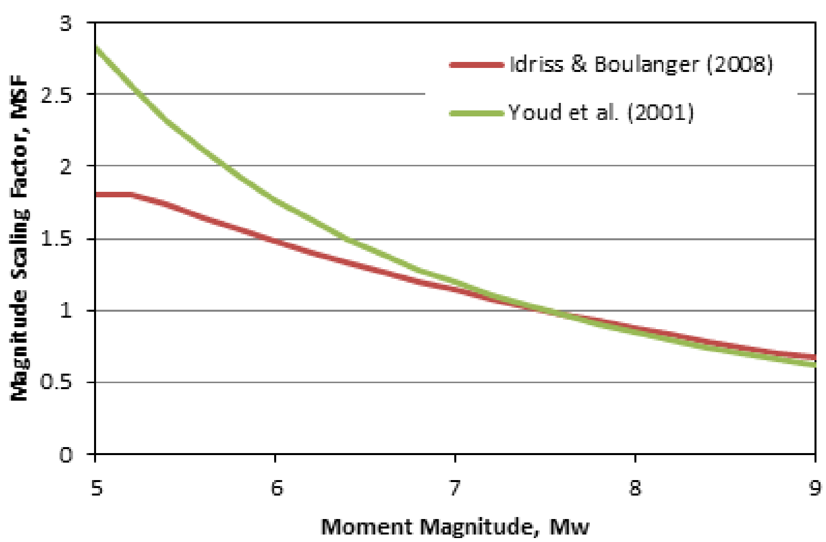

Figure 1. Comparison of Youd et al. (2001) and Idriss and Boulanger (2008) Magnitude Scaling Factors

Depth reduction factors, r_d for use with Youd et al. (2001) and Idriss and Boulanger (2008) procedures for evaluating the triggering of liquefaction are given in **Table 2**.

Table 2. Depth deduction factors for use with Youd et al. (2001) and Idriss and Boulanger (2008) procedures for predicting liquefaction triggering

NCEER Youd et al. (2001)	Idriss and Boulanger (2008)
$r_d = \frac{1-0.4113z^{0.5}+0.04052z+0.001753z^{1.5}}{1-0.4117z^{0.5}+0.05729z+0.006205z^{1.5}+0.00121z^{2}}$	$r_d = \exp[\alpha(z) + \beta(z)M_w]$ where $\alpha(z) = -1.012 - 1.126\sin\left(\frac{z}{11.73}+5.133\right)$ $\beta(z) = 0.016 + 0.018\sin\left(\frac{z}{11.28}+5.142\right)$ with z in metres and limited to a maximum depth of 20m, below which the use of site specific response analysis is recommended.

2.3 Rigorous Stress Analysis

A more rigorous approach to computing the seismic shear stresses is to use site response analysis. The analysis should be performed with a suite of input motions scaled to the uniform hazard spectrum for the site with an exceedance rate of 2% in 50 years. The number of input motions required depends on the number of different types of sources with about 10 motions per source type. The seismicity British Columbia is driven by 3 types of sources; crustal, subcrustal and subduction. The peak cyclic shear stress amplitudes at the depths of interest should be taken as the averages of the peak values produced by the site response analyses. While this is a more accurate method of getting site specific shear stresses, it was not the procedure followed in establishing the liquefaction assessment charts which ultimately form the basis for the assessment of liquefaction potential. Sometimes the differences are substantial.

Recently Boulanger et al. (2014) formulated the procedure for assessing liquefaction potential as follows:

"The formal assessment of liquefaction at a site using the simplified procedure should be based on the a_{max} that is estimated to develop in the absence of soil softening or liquefaction."

2.4 SPT-Based Resistance

SPT-based liquefaction evaluation procedures are based on the correlation of liquefaction resistance to the corrected standard penetration resistance of the soil. The correlation recommended by Youd et al. (2001) is shown in **Figure 2**. The correction process involves the application of a number of correction factors to the field measured SPT resistance. The necessary corrections are described in Youd et al. (2001). It is important to correct the SPT measurements for overburden pressure and non-plastic fines content. The overburden correction factor, C_N, is given in **Table 3** and the fines correction procedures specified by Youd et al. (2001) and Idriss and Boulanger (2008) are shown in **Table 4**.

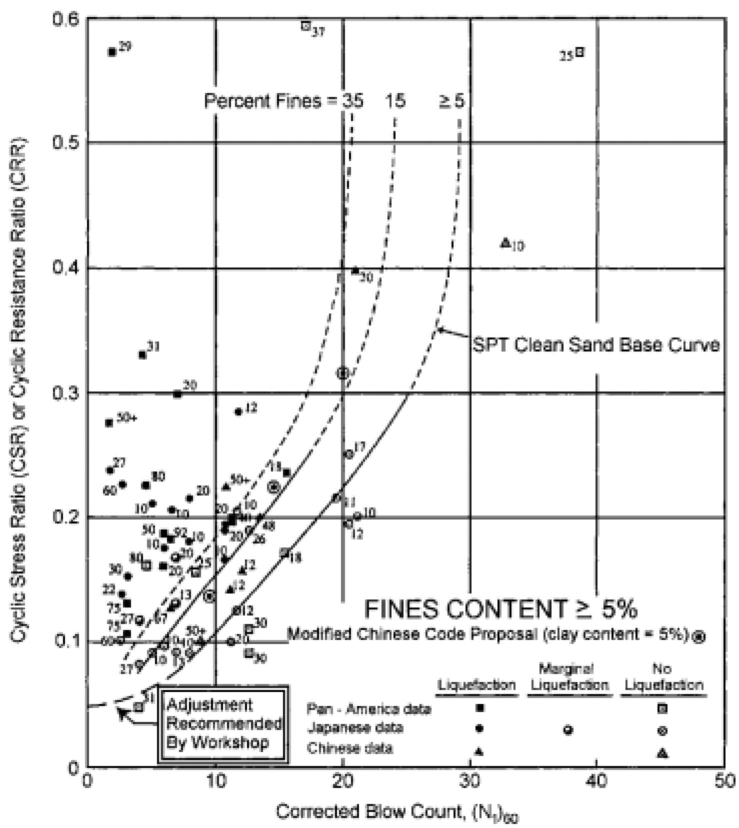

Figure 2. Liquefaction assessment hart based on normalized SPT-N values (Youd et al. 2001)

Table 3. Overburden corrections for measured SPT-N values

NCEER Youd et al. (2001)	Idriss and Boulanger (2008)
Either of the equations below may be used for overburden correction. $C_N = \sqrt{\frac{p_a}{\sigma'_{v0}}}$ $C_N = 2.2/\left(1.2+\frac{\sigma'_{v0}}{p_a}\right)$	$C_N = \left(\frac{\sigma'_{v0}}{p_a}\right)^{0.784-0.0768\sqrt{(N_1)_{60}}} \leq 1.7$ Note: Since $(N_1)_{60}$ is required to compute C_N (on which $(N_1)_{60}$ depends), iteration is required.

Table 4. Clean Sand Corrected SPT Resistance (Correction for fines content)

Youd et al. (2001)	Idriss and Boulanger (2008)
$(N_1)_{60,cs} = \alpha+\beta(N_1)_{60}$ where $\alpha = \begin{cases} 0 & , FC \leq 5\% \\ \exp[1.76-\frac{190}{FC^2}], & 5\% < FC < 35\% \\ 0 & , FC \geq 35\% \end{cases}$ $\beta = \begin{cases} 1.0 & , FC \leq 5\% \\ 0.99-\frac{FC^{1.5}}{1000}, & 5\% < FC < 35\% \\ 1.2 & , FC \geq 35\% \end{cases}$ and FC is in percent.	$(N_1)_{60,cs} = (N_1)_{60}+\Delta(N_1)_{60}$ where $\Delta(N_1)_{60} = \exp\left[1.63+\frac{9.7}{FC+0.01}-\left(\frac{15.7}{FC+0.01}\right)^2\right]$ and FC is in percent.

The equations for calculating the cyclic resistance ratios, CRR @ $\sigma = 1_{atm}$ as functions of $(N_1)_{60,cs}$ using the Youd and Idriss& Boulanger procedures, are given in **Table 5**.

Table 5. Cyclic Resistance Ratios (CRR) for M = 7.5 and σ'_{vo} = 1atm

NCEER Youd et al. (2001)	Idriss and Boulanger (2008)
$CRR_{\sigma'=1atm} = \frac{1}{34-(N_1)_{60,cs}} + \frac{(N_1)_{60,cs}}{135} + \frac{50}{(10(N_1)_{60,cs}+45)^2} - \frac{1}{200}$	$CRR_{\sigma'=1atm} = \exp\left[\frac{(N_1)_{60,cs}}{14.1} + \left(\frac{(N_1)_{60,cs}}{126}\right)^2 - \left(\frac{(N_1)_{60,cs}}{23.6}\right)^3 + \left(\frac{(N_1)_{60,cs}}{25.4}\right)^4 - 2.8\right]$

The Youd et al. (2001) and Idriss and Boulanger (2008) procedures require that the value of CRR be adjusted to account for the in- situ vertical effective stress using the relationships.

$$CRR\ @\ \sigma' = K_\sigma\ CRR\ @\ \sigma'=1atm \qquad (\mathbf{2})$$

The expressions for K_σ are shown in **Table 6**.

Table 6. Overburden stress correction factor, K_σ, for SPT- and CPT-Based methods

NCEER Youd et al. (2001)	Idriss and Boulanger (2008)
$K_\sigma = \min\begin{cases}\left(\frac{\sigma'_{v0}}{p_a}\right)^{f-1}\\ 1.0\end{cases}$ where f = 0.7-0.8 for D_r = 40-60% and f = 0.6-0.7 for D_r = 60-80%.	$K_\sigma = \min\begin{cases}1-C_\sigma \ln\left(\frac{\sigma'_{v0}}{p_a}\right)\\ 1.1\end{cases}$, where $C_\sigma = \frac{1}{18.9-2.55\sqrt{(N_1)_{60}}} \le 0.3$ for SPT $C_\sigma = \frac{1}{17.3-8.27\sqrt{q_{c1N}^{0.264}}} \le 0.3$ for CPT

The correlation of CRR for σ'=1atm and magnitude M=7.5 with normalized SPT-N is shown in **Figure 3**. Both the Youd et al. (2001) and Idriss and Boulanger (2008) procedures give very similar results for M=7.5 when MSF=1.0. However for M=6.0, the different approaches to scaling factors result in significantly different CRR correlations with $(N_1)_{60}$ .as shown in **Figure 4**. The impact of the different scaling factors will be noticeable primarily for sources with M_{ma} ≤6.5.

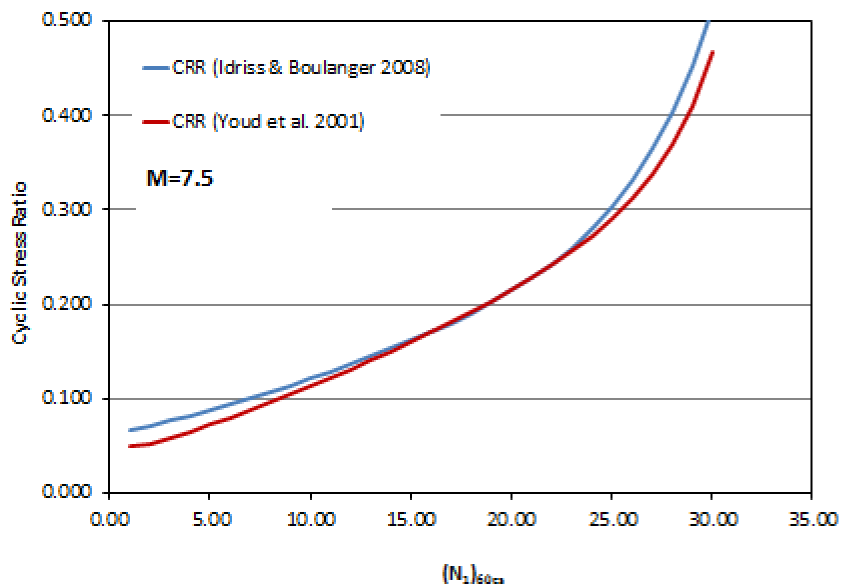

Figure 3. Liquefaction resistance curves for M=7.5 by Youd et al. (2001) and Idriss and Boulanger (2008) procedures

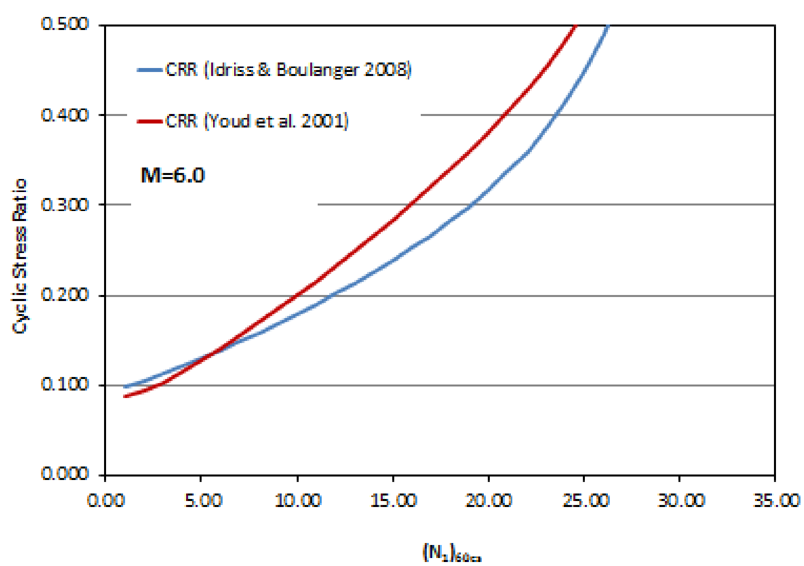

Figure 4. Liquefaction resistance curves for M=6.0 by Youd et al. (2001) and Idriss and Boulanger (2008) procedures

The Youd et al. (2001) and Idriss and Boulanger (2008) equations for correcting normalized SPT values for fines content seem to give similar results as shown in **Figure 5** for M = 7.5 and σ'_{v0} = 1atm**.**

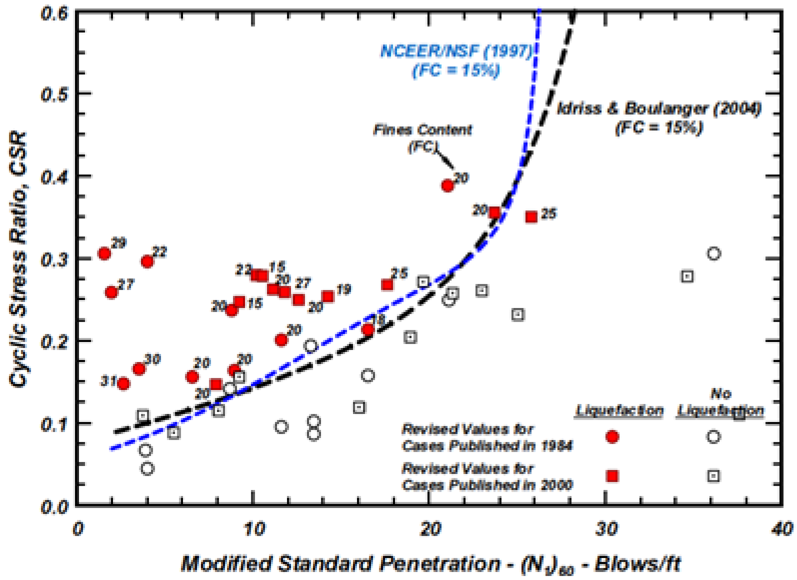

Figure 5. SPT case histories of cohesionless soils with 15%≤FC<35% and the Idriss and Boulanger (2008) and the Youd et al. (2001) curves for FC=15% for *M*=7½ and σ'$_{v0}$=1atm

2.5 CPT-Based Resistance

CPT-based liquefaction evaluation procedures are based on the correlation of liquefaction resistance with normalized cone penetration resistance q_{c1N}. The most recent correlation which has been recommended by Idriss and Boulanger (2006) is shown in **Figure 6**. The normalization factor, C_N, is given in **Table 7**.

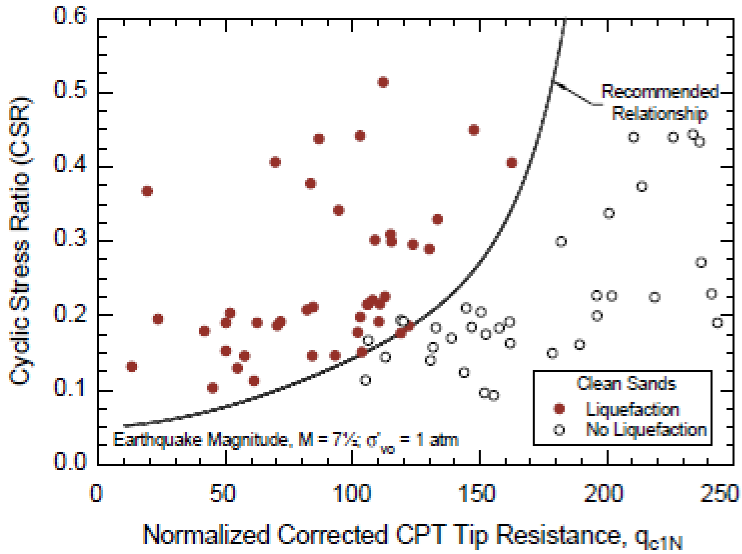

Figure 6. Liquefaction assessment chart based on normalized cone bearing pressure (Idriss and Boulanger (2008).

Table 7. Overburden corrections for measured CPT-N values

NCEER Youd et al. (2001)	Idriss and Boulanger (2008)
Either of the equations below may be used for overburden correction. $q_{c1N} = C_Q \frac{q_c}{p_a}$ where $C_Q = \frac{p_a}{\sigma'_{v0}}^{n}$ And n is an exponent that varies with soil type with a value of between 0.5 and 1.0.	$C_N = \left(\frac{p_a}{\sigma'_{v0}}\right)^{1.338-0.249(q_{c1})^{0.264}} \leq 1.7$ Note: Since q_{c1} is required to compute C_N (on which q_{c1} depends), iteration is required.

The CRR for clean sand in terms of q_{c1N} are given by equation

$$CRR_{\sigma'=1atm} = \exp\left[\frac{q_{c1N}}{540} + \left(\frac{q_{c1N}}{67}\right)^2 - \left(\frac{q_{c1N}}{80}\right)^3 + \left(\frac{q_{c1N}}{114}\right)^4 - 3\right] \quad (3)$$

The effects of non-plastic fines on liquefaction resistance are taken into account by modifying q_{c1N} according to **Equation (4)**.

$$q_{c1Ncs} = q_{c1N} + \Delta q_{c1N} \quad (4)$$

where

$$\Delta q_{c1N} = \left(5.4 + \frac{q_{c1N}}{16}\right) \times \exp\left[1.63 + \frac{9.7}{FC+0.01} - \left(\frac{15.7}{FC+0.01}\right)^2\right] \quad (5)$$

The CPT- based liquefaction resistances, CRR, for various fines contents are shown in **Figure 7.**

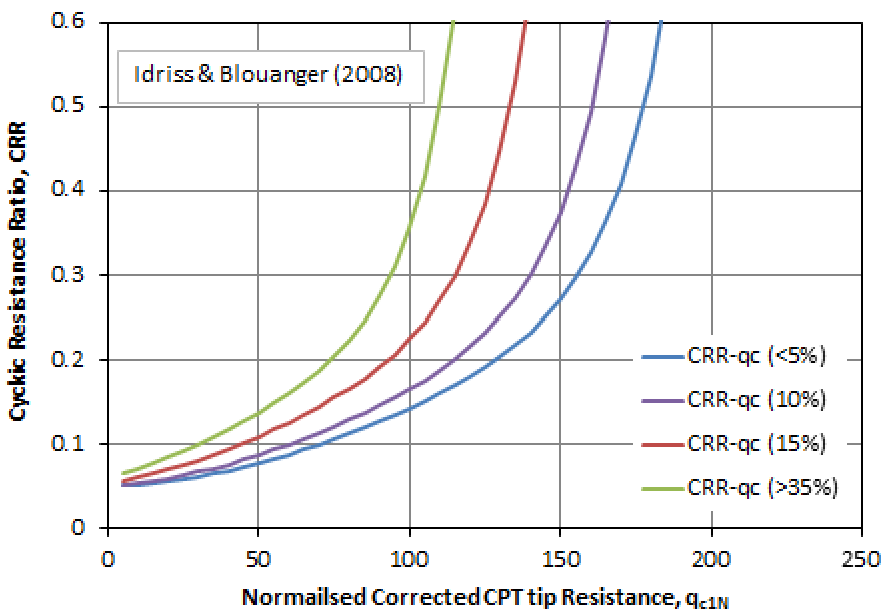

Figure 7. Correlation of liquefaction resistance with normalized CPT data for various fines contents.

2.6 V_s-Based Resistance

The database supporting the use of a V_s based correlation with CRR has been summarized by Andrus and Stokoe (2000) and Andrus et al. (2003). The V_s method is used mostly in soils which are difficult to penetrate or sample such as gravels. It is the least sensitive of the methods for evaluating liquefaction, especially in differentiating the effects of various fines contents. This is clear from the correlation chart shown in **Figure 8**.

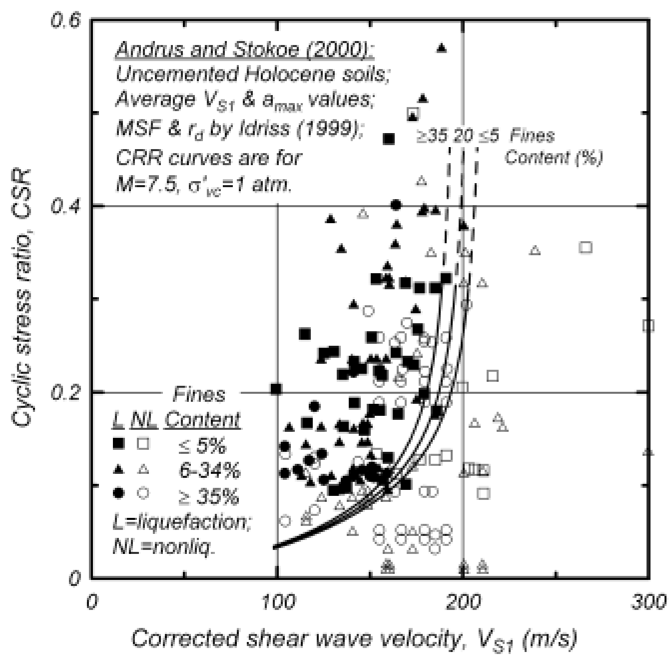

Figure 8. V_s-based Liquefaction correlation for clean uncemented sands (after Andrus & Stokoe 2000)

Idriss and Boulanger (2008, pp115-116) give a helpful brief assessment of the merit of the V_s procedure relative to SPT and CPT procedures.

A convenient and economic method for estimating the shear wave velocity, V_s, is to invert ambient vibration data to achieve the best estimate of the V_s profile of the site. The best estimate is the average profile resulting from about 100,000 Monte Carlo realisations as shown in **Figure 9**. The figure gives the mean, which is the profile normally used for liquefaction assessment but also gives and idea of the range of the computed data. The agreement with measured downhole data is very good. Filled circles depict averaged down-hole and SCPT measurements to 60m depth. Open circles depict averaged down-hole only measurements.

Average relative difference in V_S is 5% between average geotechnical data and inversion result to 110m depth.

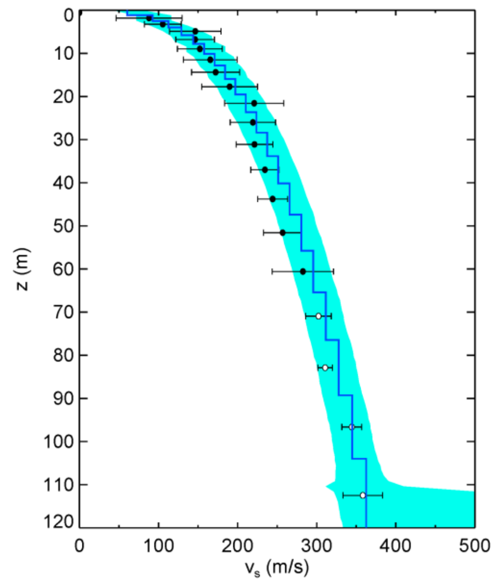

Figure 9. V_s-based Liquefaction correlation for clean uncemented sands (after Andrus & Stokoe 2000)

Figure 10 shows the results of liquefaction assessments at four boreholes, one of which goes to a depth of 300m. The round yellow points come from the ambient vibration velocity and the other points come from the downhole velocities. It is clear that within the range probed by the ambient velocity that the results compare very favourably with the downhole velocity results. The method seems to be quite reliable.

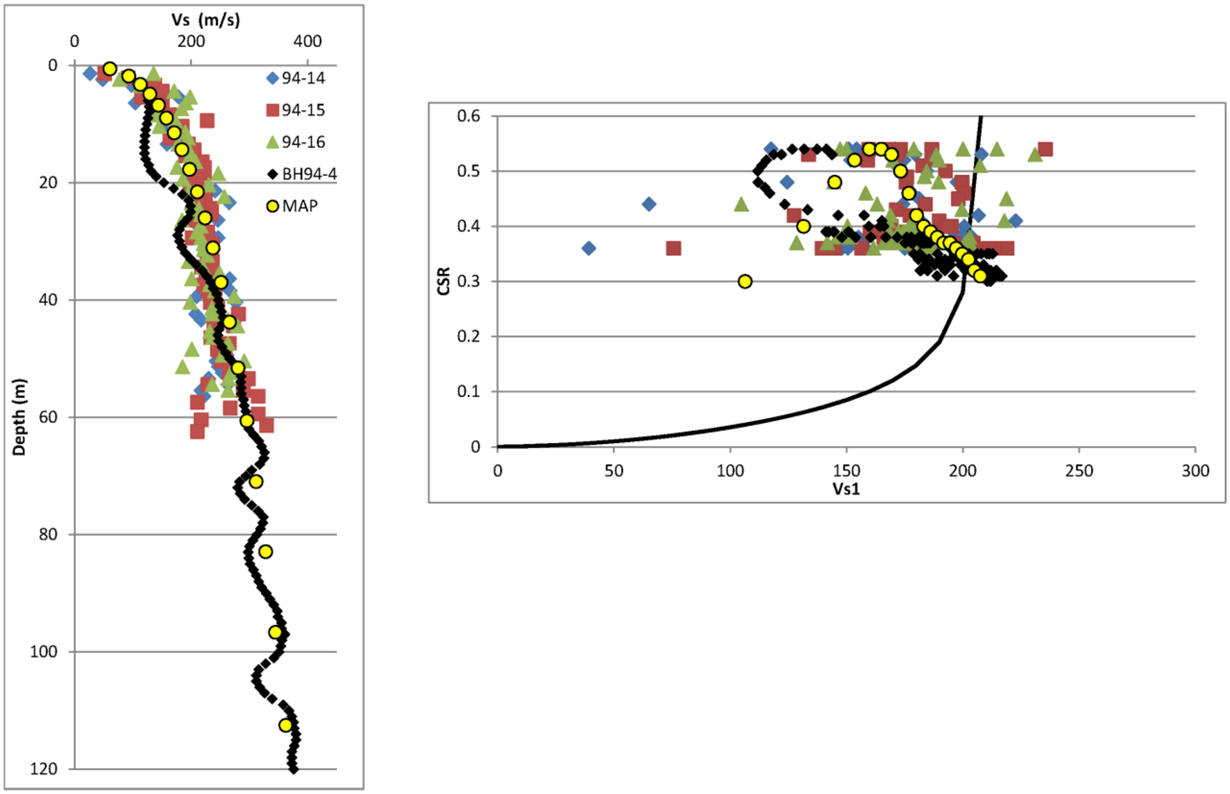

Figure 10. V_s-based Liquefaction correlation for clean uncemented sands (after Andrus & Stokoe 2000)

2.7 Liquefaction Assessment Software

There is some very useful and cheap software available for evaluating liquefaction potential and its consequences especially for the CPT assessment.

A sample output is given in **Figure 11**. The distribution of CRR and seismic demand is in the first cell, followed by distribution of the factor of safety with depth in the second cell. The third cell shows the distribution of the liquefaction potential index. The last two cells show the vertical distributions of lateral displacements and settlements.

The Liquefaction Potential Index, LPI, is defined as

$$LPI = \int_{0}^{20} F(z).w(z)dz \qquad (6)$$

where z is depth of the midpoint of the sublayer under consideration (0 to 20 m) and dz is an increment in depth. The liquefaction potential gives greater weight to layers which liquefy near the surface, than those at depth, and therefor gives a good overall assessment of the site. The weighting factor, w(z), and the severity factor, F(z), are calculated follows:

- $F(z) = 1 - FS$ for $FS < 1.0$
- $F(z) = 0$ for $FS \geq 1.0$
- $w(z) = 10 - 0.5z$ for $z < 20$ m
- $w(z) = 0$ for $z > 20$ m

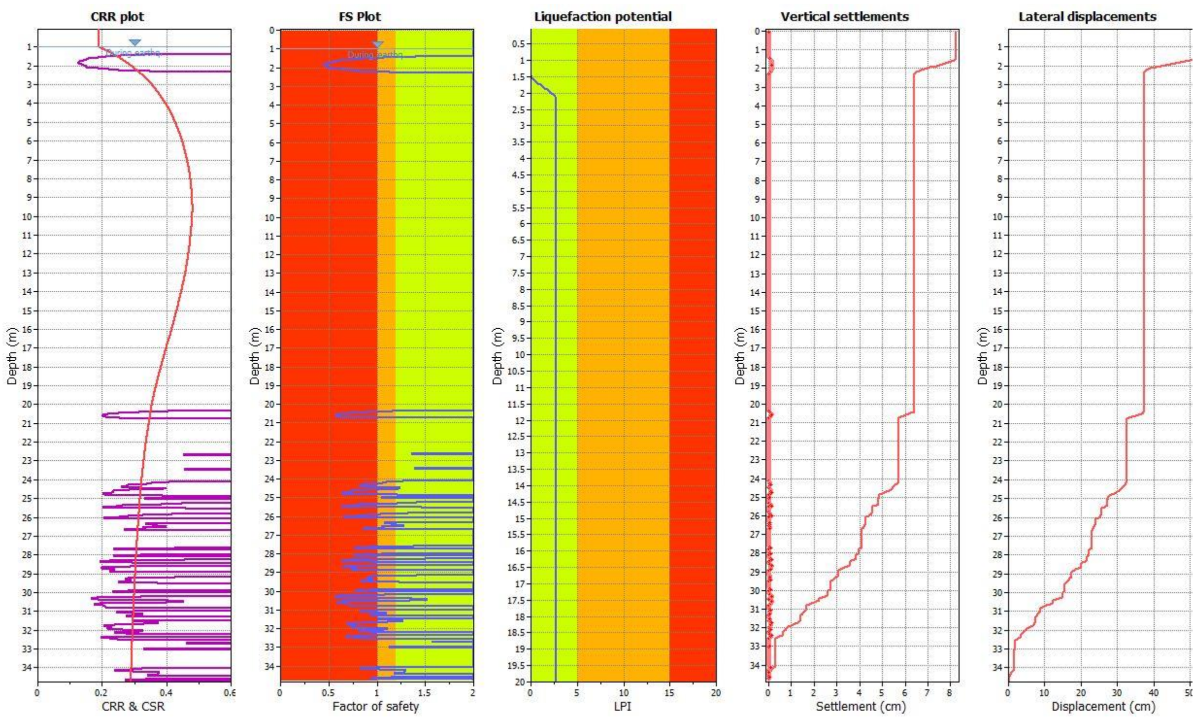

Figure 11. Liquefaction analysis of CPT data using CLIQ software

2.8 Simplified Method using Probabilistic Accelerations

The simplified methods described above are deterministic. The seismic hazard at the site is based on a known pair of parameters, M and a_{max}. Therefore the MSF for M can be applied directly in **Equation (1 bis).**

$$CSR = 0.65 \frac{a_{max}}{g} \cdot \frac{\sigma_{v0}}{\sigma'_{v0}} \cdot \frac{r_d}{MSF} \qquad \textbf{(1 bis)}$$

However, if a probabilistic PGA is used, which is the result of the contributions of many magnitudes to PGA, what magnitude and hence what MSF should be used? In current practice a single magnitude is often selected which tends towards the maximum magnitude expected in the governing seismic source zone and its weighting factor is used with the NBCC 2010 PGA. In

Vancouver prior to 2007 M=7.3 was recommended for use. In 2007 M=7.0 was suggested. .Does these suggested magnitudes represent adequately the combined effects of the many different magnitudes contributing to the probabilistic PGA? The answer to this question is not a matter of opinion but can be demonstrated directly by two independent methods: (1) a probabilistic seismic hazard analysis using weighted magnitudes and (2) a procedure based on a magnitude - distance deaggregation for the BC code hazard level of a 2% exceedance rate in 50 years. The weighted magnitude probabilistic analysis approach is described in detail by Finn & Wightman (2007). It requires access to a seismic hazard analysis program. The deaggregation method is easy to implement because the magnitude – distance deaggregation is available from USGS. Finn & Wightman (2007) have shown that both methods give the same results.

2.9 Weighted Residual Method

The weighted magnitude probabilistic analysis approach was first proposed by Idriss (1985). He demonstrated the need for weighting the magnitudes and showed how for the same acceleration level the return period for the weighted response could be much longer depending on the seismic environment. The weighting factors, MWF, used in the study by Idriss are the inverse of the MSF proposed by Youd et al. (2001).

The weighted magnitude probabilistic analysis is accepted in California as a procedure for implementing the requirements of the Division of Mines and Geology guidelines in DMG SP 117 and the Seismic Mapping Act for projects requiring review under the Seismic Mapping Act of California. DMG SP 117 states "The alternative approach calculating "magnitude-weighted accelerations" is considerably easier and it provides a unique magnitude to be used with the probabilistically derived accelerations" (SCEC 1999).

The weighted magnitude probabilistic analyses reported in this paper were conducted to obtain the magnitude–acceleration pair for evaluating liquefaction potential. In this context, the weighted hazard curves are called liquefaction hazard curves. The seismic hazard curve for Vancouver and the corresponding liquefaction hazard curve weighted for magnitude M = 7.5 are shown in **Figure 12**.

The acceleration for assessing liquefaction potential for an exceedance rate of 2% in 50 years is 0.30g for M=7.5 and the site factor C=1.0. For other values of C, the compatible acceleration is 0.30g. The liquefaction hazard acceleration should be used directly with the liquefaction resistance curve for magnitude M=7.5 without further scaling. As pointed out by Idriss (1985) the weighted probabilistic analysis can be done for any normalizing earthquake magnitude other than M=7.5 but the appropriate magnitude weighting factor for the chosen normalizing magnitude must be applied again, when calculating liquefaction resistance using **Figure 2**. Therefore, when evaluating liquefaction triggering only, the magnitude-acceleration pair to be used is the normalizing magnitude and the associated weighted acceleration.

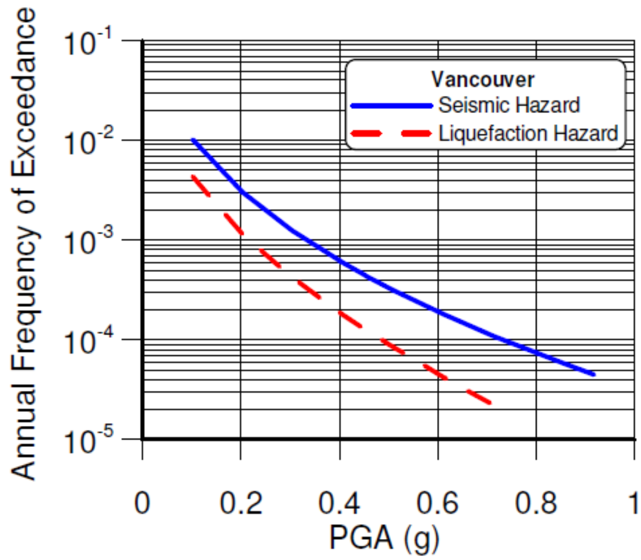

Figure 12. Liquefaction and acceleration curves for Vancouver normalized for M = 7.5

The unweighted and weighted PGA are for firm ground and, depending on the intensity of shaking, will be amplified or deamplified at the surface by a site factor C on propagating through the softer soils often associated with liquefaction. The site factor C is usually determined by an appropriate site response analysis. Other options that are used are generalized amplification data such as provided in Idriss (1990), or the short period amplification factors in NBCC 2005. The factors of safety against liquefaction presented in the following were calculated by the simplified method for a range in $(N_1)_{60}$ values using the magnitude-acceleration pair from the weighted magnitude probabilistic analysis. Generic site conditions were assumed, consisting of sand, with unit weight 20 kN/m^3, a water table at 2m, and a range of $(N_1)_{60}$ values at 6m depth. For these analyses the site factor was assumed to be C=1. The factors of safety are shown in **Table 8**.

Current practice in Vancouver for evaluating liquefaction potential is to use the NBCC 2005 accelerations with a magnitude M = 7.3. The factors of safety from this approach are also given in **Table 8**.

Table 8. Factors of safety against liquefaction for Vancouver

SPT Blowcount, $(N_1)_{60}$	**Liquefaction Triggering Safety Factors for Vancouver**	
	Current Practice Weighted	Magnitude Analysis
	M7.3:0.46g	M7.5:0.30g
10	0.28	0.40
13	0.35	0.49
15	0.39	0.57
18	0.47	0.67
20	0.53	0.76
25	0.72	1.02
30	1.15	1.64

Over the range $10 \leq (N_1)_{60} \leq 30$, the factors of safety from the weighted magnitude probabilistic analysis are about 43% greater than the factors given by current practice in Vancouver. If the magnitudes are weighted relative to M = 7.3, the recommended magnitude for Vancouver, the weighted magnitude probabilistic analysis gives a liquefaction acceleration of 0.35g. When M =7.3 (with MSF = 1.07) and a_{max} =0.35g are used in the simplified liquefaction assessment procedure, the factors of safety are similar to those shown for M = 7.5 and a_{max} =0.30g in **Table 8**.

2.10 Magnitude Deaggregation Method

The magnitude deaggregation method will be explained with reference to the magnitude-distance deaggregation for Vancouver shown in **Figure 13** (Halchuk & Adams 2006). In this case the magnitudes are collected in bins 0.25M wide and the central magnitude value is assigned to the bin. For example the bin labeled M=5.125 contains all earthquakes in the range 5.0 ≤ M < 5.25. The contributions of the bin magnitude to the site acceleration are sampled at various distances from the site. These contributions are shown by the row numbers in the magnitude contribution matrix in **Figure 14.**

The contributions are given per mil (1000) for convenience and are divided by 10 to give the percent contribution. The total contributions per magnitude bin are obtained by summing the distance contributions horizontally. The cumulative per cent contributions per magnitude bin are shown in the 2-D plot in **Figure 15**. The sum of the bin contributions is 100%.

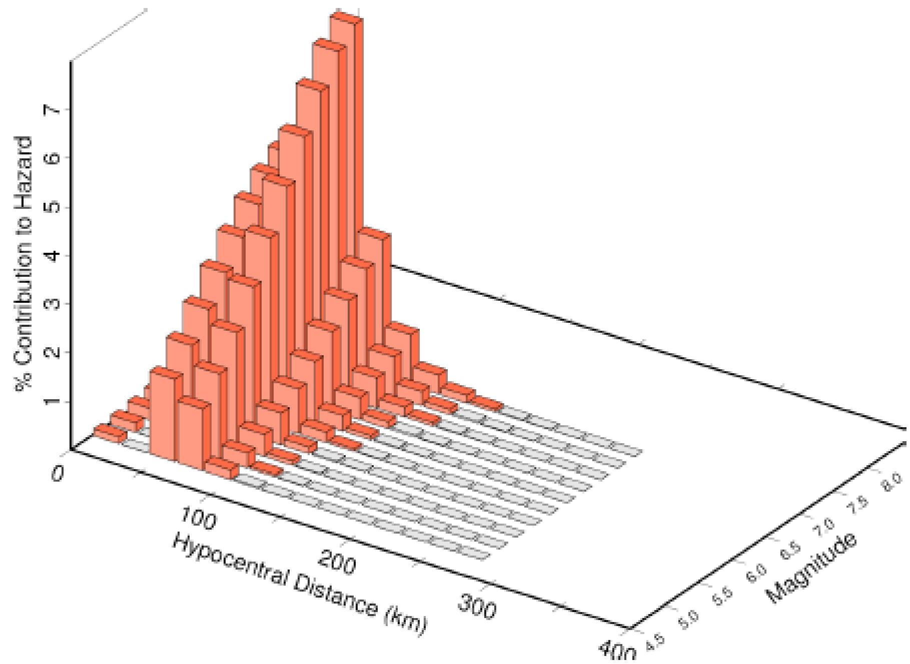

Figure 13. Magnitude-distance deaggregation for NBCC 2005 PGA in Vancouver

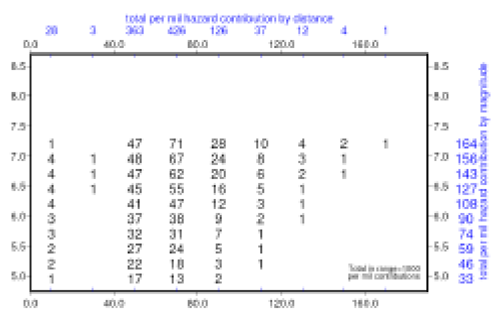

Figure 14. Deaggregation matrix for NBCC 2005 PGA in Vancouver

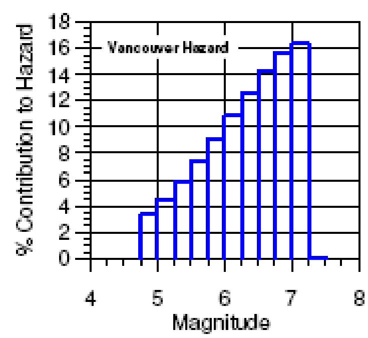

Figure 15. Magnitude Contributions to NBCC 2005 PGA Hazard in Vancouver

The factor of safety against liquefaction at a site, taking into account the magnitude scaling factors is calculated as follows. The factor of safety of the site at the code acceleration level is computed for each binned magnitude and then multiplied by the contribution of the magnitude to the site acceleration. The sum of all the contributions to the factor of safety gives the global factor of safety for the site. The calculation process for Vancouver is shown by the example in **Table 9**.

Table 9. Sample calculation for factor of safety against liquefaction for Vancouver site with $(N_1)_{60}$=18 at 6m depth

Magnitude Bins	Central Magnitude	Contribution Factor	Liquefaction S.F.	S.F. Contribution
4.75 – 5.0	4.875	0.033	1.33	0.044
5.0 – 5.25	5.125	0.045	1.17	0.052
5.25 – 5.5	5.375	0.058	1.03	0.060
5.5 – 5.75	5.625	0.074	0.92	0.068
5.75 – 6.0	5.875	0.091	0.82	0.075
6.0 – 6.25	6.125	0.109	0.74	0.080
6.25 – 6.5	6.375	0.126	0.67	0.084
6.5 – 6.75	6.625	0.143	0.60	0.086
6.75 – 7.0	6.875	0.157	0.55	0.086
7.0 – 7.25	7.125	0.163	0.50	0.082
	Sum 1.000		**Total Factor of Safety = 0.72**	

The factors of safety from the deaggregation method are compared in **Table 10** with the factors obtained using the magnitude-acceleration pair from the magnitude weighted probabilistic analysis. The factors given by previous (M=7.3) and current practice (M=7.0) in Vancouver and those arising from using mean and modal magnitudes with the code acceleration are also shown. The mean magnitude, deaggregation and weighted magnitude methods give factors of safety within an average of 2% of each other. The simplest approach seems to be the mean magnitude combined with the estimated peak ground acceleration for the appropriate hazard level.

Table 10. Factors of safety against liquefaction in Vancouver for various triggering options

SPT Blow-Count $(N_1)_{60}$	Modal Magnitude (M7.1: 0.46g)	Current Practice (M=7.0)	Mean Magnitude (M6.3: 0.46g)	Deaggregation Method (M7.25-4.75: 0.46g)	Weighted Magnitude Analysis (M7.5: 0.30g)
10	0.30	0.32	0.40	0.41	0.40
13	0.37	0.39	0.50	0.51	0.49
15	0.42	0.44	0.57	0.58	0.57
18	0.50	0.53	0.68	0.72	0.67
20	0.56	0.59	0.77	0.78	0.76
25	0.76	0.81	1.04	1.05	1.02
30	1.22	1.29	1.66	1.69	1.64

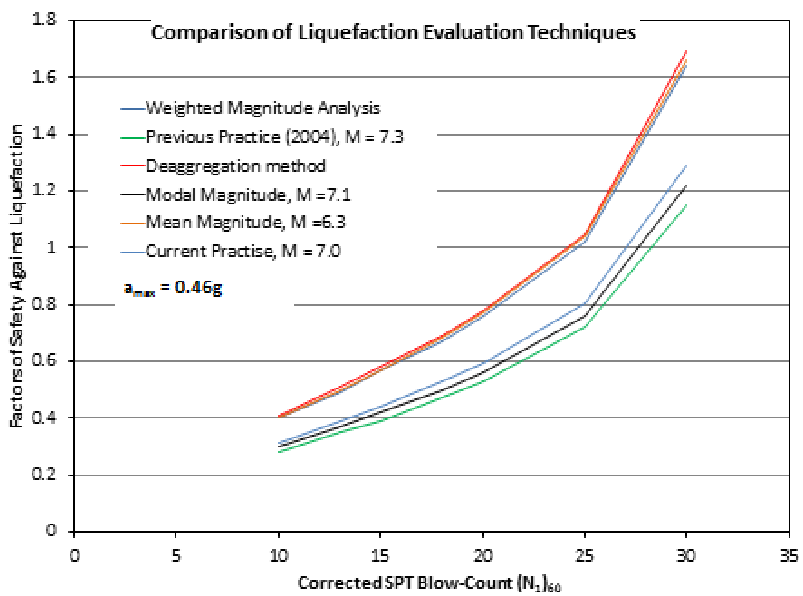

Figure 16. Liquefaction potential for various $(N_1)_{60cs}$ values and seismic site conditions, using Youd et al. (2001)

The analyses were repeated for a peak ground acceleration of 0.35g, which was obtained by site response analysis. The factors of safety were evaluated by the deaggregation, mean magnitude and using current practice with M=7.0 and PGA=0.35g. The results are shown in **Figure 16**.

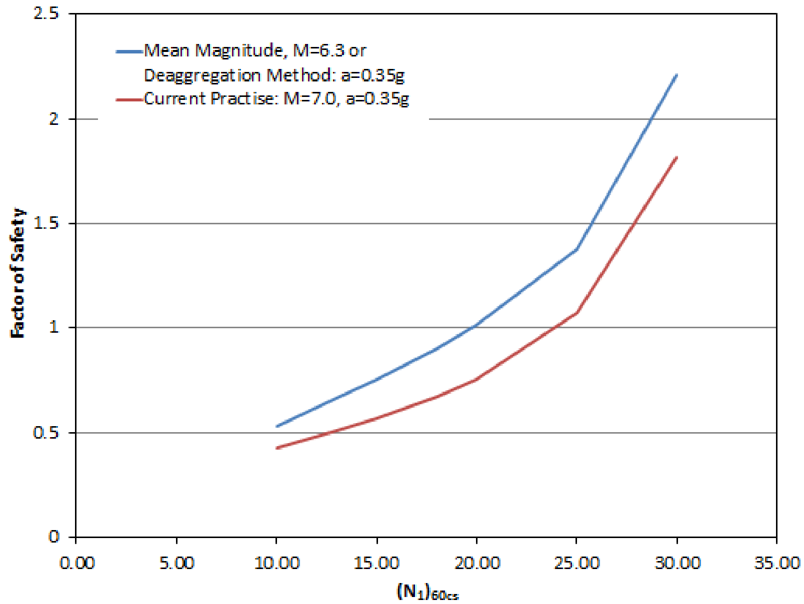

Figure 17. Liquefaction potential for various $(N_1)_{60cs}$ values and a_{max}=0.35g, using Youd et al. (2001)

3.0 Liquefaction or Cyclic Failure of Fine-Grained Clays and Plastic Silts

3.1 Simplified Stress Analysis for Plastic Soils

The cyclic failure of clays and plastic silts depends on the balance between seismic demand and resistance capacity. As in the case of sands, the Simplified Procedure by Seed and Idriss (1971) will be used to estimate the seismic demand in terms of the cyclic stress ratio, CSR given by **Equation (1 bis).**

$$CSR = 0.65\frac{a_{max}}{g}\cdot\frac{\sigma_{v0}}{\sigma'_{v0}}\cdot\frac{r_d}{MSF} \qquad \textbf{(1 bis)}$$

The magnitude scaling factor, MSF, is defined as

$$MSF = \frac{CRR_M}{CRR_{M=7.5}} \qquad (\mathbf{7})$$

The MSF is used to convert a cyclic stress ratio due to a given magnitude, M, to the equivalent stress ratio for M=7.5. The cyclic behavior of plastic soils is very different from that of sands and so the equivalent stress ratios will be different. Boulanger and Idriss (2004) developed MSF for plastic soils to facilitate the application of the Simplified Method to clays and plastic silts. Their report presents a careful, fundamental analysis of the cyclic behavior of plastic soils and deserves detailed study. The MSF for clay is given by

$$MSF = 1.12\exp\left(^{-M_w}/_4\right) - 0.828 \qquad (\mathbf{8})$$

with the MSF clay ≤ 1.13 compared with the MSF sand ≤ 1.8.

MSF clay is plotted in **Figure 18**. The MSF for sand is shown for comparison. The variation of MSF clay with magnitude is quite flat. Values range from a maximum value of 1.13 at Mw=5.0 to approximately 1.0 at Mw = 8.5. The corresponding range for sands is 1.18 – 0.8.

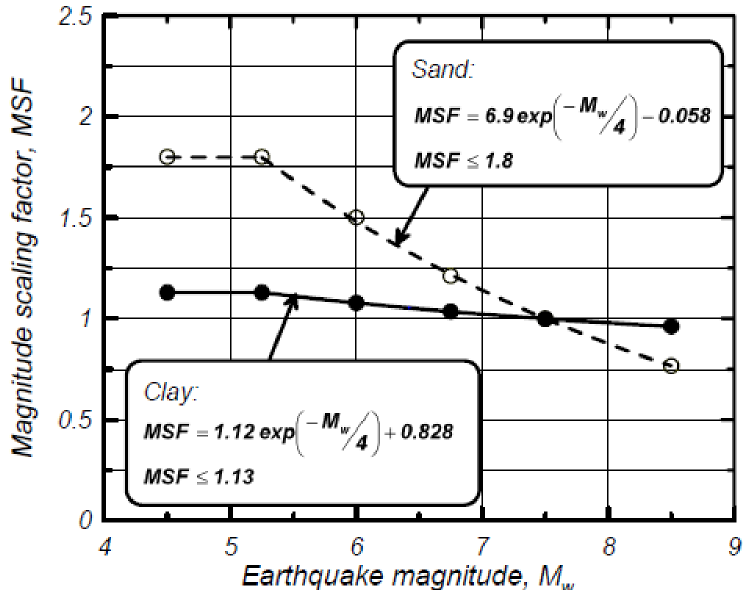

Figure 18. Magnitude scaling factors for converting a cyclic stress ratio due to a magnitude, M, to the equivalent cyclic stress ratio for M = 7.5 for sand like and clay like soils (Boulanger and Idriss, 2004)

3.2 Resistance Capacity, CRR

The cyclic resistance ratio, CRR, for cohesionless soils has been established as a function of normalized quantities: SPT-N, Q_c and V_s and therefore can be determined from routine in situ field measurements. A similar data base is not available for clays. There are 3 recognized methods for determining CRR for clays (Boulanger and Idriss, 2004):

1. The direct method using cyclic loading tests on high quality samples

2. Measure the monotonic undrained shear strength, S_u, in situ or by test on high quality samples

3. Estimate Su based on the stress history of the soil profile

Method 1.

The proper use of Method 1 requires that state of practice protocols for sampling and testing be followed.

Method 2.

The vane shear test, VST, provides the best estimate of S_u, by in situ methods. It also allows the determination of residual strength, S_r, and therefore gives a measure of the Sensitivity of the clay:

$$S = \frac{S_u}{S_r} \quad \textbf{(9)}$$

The measured S_u has to be adjusted to field value using a correction factor μ (Bjerrum, 1972) giving:

$$(M_u)_{field} = \mu(S_u)_{VST} \quad \textbf{(10)}$$

The μ factor is in **Figure 19** as a function of PI.

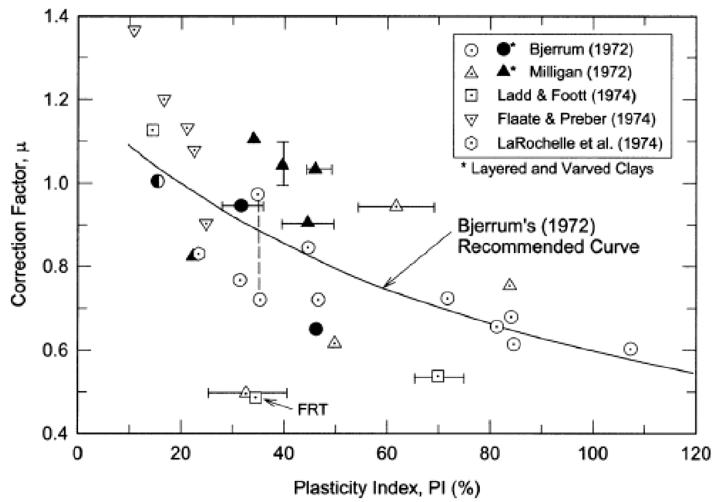

Figure 19. Correction factor μ for VST measurements of undrained strength (Ladd and DeGroot 2003, after Ladd et al. 1977)

The undrained strength can be estimated from CPT tip resistance by the relation:

$$S_u = \frac{(q_{ct} - \sigma_v)}{N_k} \quad \textbf{(12)}$$

N_k can have a range of 10-30 but for normally consolidated and lightly over-consolidated clays a value of N_k = 14 is often used.

3.3 Estimating CRR from S_u Profile

The CRR when M = 7.5 can be estimated for S_u profiles obtained by either Method 1 or 2 using **Equation (13)**.

$$CRR_{M = 7.5} = (\tau_{cyc}/S_u)_{N = 30}\ (S_u/\sigma^i_{vc}) \tag{13}$$

The cyclic shear stress τ_{cyc} is 65% of the peak shear stress as for sand but the ratio $(\tau_{cyc}/S_u)_{N = 30}$ is evaluated from a substantial data base for N = 30 cycles when M = 7.5. The value 0.83 was selected for clay-like soils subjected to direct simple shear loading conditions. This value may change as more data as more data becomes available. For the present, CRR is given by **Equation (14)**:

$$CRR_{clay} = 0.83\ (S_u/\sigma^i_{vc}) \tag{14}$$

If a correction factor $C_{2D} = 0.96$ is included to represent the fact that motions occur in the field in two directions then:

$$CRR_{clay} = 0.8\ (S_u/\sigma^i_{vc}) \tag{15}$$

3.4 Method 3

The CRR may also be estimated from the stress history of the soil profile i.e. the consolidation history. The undrained shear strength may be related to σ^i_{vc} and OCR as follows:

$$S_u/\sigma^i_{vc} = S.\ OCR^m \tag{16}$$

Then from **Equation (15)** the CRR is given by:

$$CRR_{M = 7.5} = 0.8\ S\ OCR^m \tag{17}$$

Based on research by Ladd (1991), Boulanger and Idriss (2004) recommended S = 0.22 and m = 0.8 for homogeneous, low to high plasticity, sedimentary clays. Then:

$$CRR_{M = 7.5} = 0.18\ OCR^{0.8} \tag{18}$$

3.5 Effect of Initial Static Shear Stress

As in the case of sand the CRR is affected by the presence of an initial static shear stress when the site is sloping**.** In this case the level ground CRR must be multiplied by the slope factor Kα. The Kα. is shown in **Figure 20** as a function of the initial static shear stress ratio α and the over-consolidation ratio OCR.

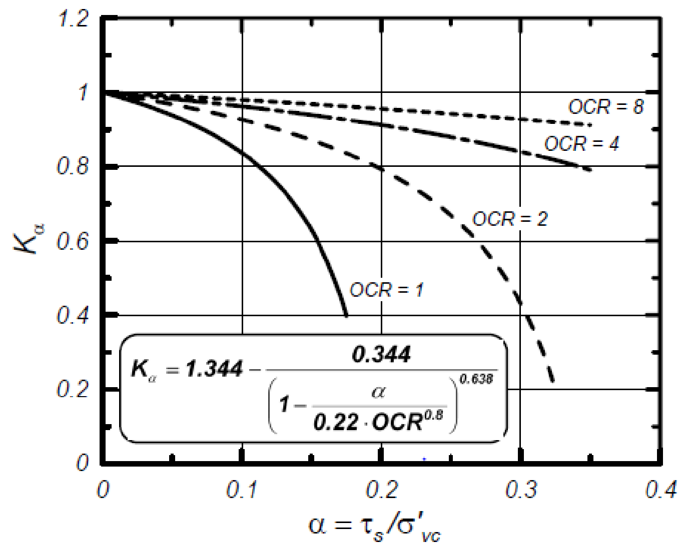

Figure 20. The slope correction factor Kα as a function of initial static shear stress ratio and OCR

3.6 Consequences of Cyclic Failure in Plastic Soils

Unlike the case of sands, there are no empirical formulas to estimate lateral spreading in clay-like soils. Boulanger and Idriss (2004) and Idriss and Boulanger (2008) suggest using the Newmark sliding block analysis to estimate deformations on potential sliding surfaces. The shear strength may be the remolded strength or a strain depend shear strength may be used. The Newmark method assumes a rigid block sliding on a failure surface. If a significant volume of soils is involved in the sliding failure the displacement are likely to be underestimated. A nonlinear site response analysis will give an estimate of the distribution of shear strains in the vertical direction and provide the basis for estimating lateral spreading,

4.0 Consequences of Liquefaction in Terms of Ground Displacements

4.1 General

Broadly speaking there are 2 approaches in common use for estimating the amount of lateral spreading in liquefiable ground for school projects, once the possibility of flow failure is eliminated. The first class of methods is exemplified by Youd et al. (2002) who assembled a database of lateral spreading observations and developed regression equations for lateral spread prediction, based on geotechnical profile information and the magnitude and distance of the triggering event. The second class of methods uses laboratory data from simple shear testing and shake table testing to arrive at cyclic strain limits once liquefaction is triggered in materials of various initial densities (and field penetration resistance). The lateral displacements are the calculated from the strains. Idriss and Boulanger (2008, pp 133-135) give a very lucid description of the various shear strain based methods.

4.2 Youd et al. (2002) Model

Bartlett and Youd (1995) compiled a large database of lateral spreading case histories from Japan and the western United States and developed a regression-based predictive relationship. Youd et al. (2002) used an expanded and corrected version of the 1992 database to develop the predictive relationship for displacement. The database is illustrated in **Figure 21**.

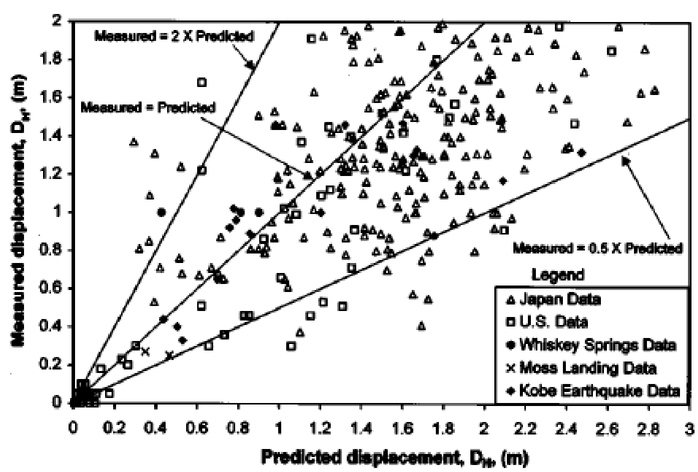

Figure 21. Measured versus predicted displacements for displacements of up to 2m

The displacement for given seismic and site conditions is given by **Equation 19**.

$$\log D_H = b_0 + b_1 Mw + b_2 \log R^* + b_3 R + b_4 \log W + b_5 \log S + b_6 \log T_{15} + b_7 \log(100 - F_{15}) + b_8 \log(D50_{15} + 0.1 \text{ mm}) \qquad (\mathbf{19})$$

where D_H = horizontal displacement in meters and $R^* = R + 10 - 0.89Mw - 5.64$. The values of the coefficients are presented in **Table 11**.

Table 11. Coefficients for Youd et al. (2002) predictive equation

Model	b_0	b_1	b_2	b_3	b_4	b_5	b_6	b_7	b_8
Ground slope	-16.213	1.532	-1.406	-0.012	0	0.338	0.540	3.413	-0.795
Free face	-16.713	1.532	-1.406	-0.012	0.592	0	0.540	3.413	-0.795

The geometric parameters of the site are shown in **Figure 22**.

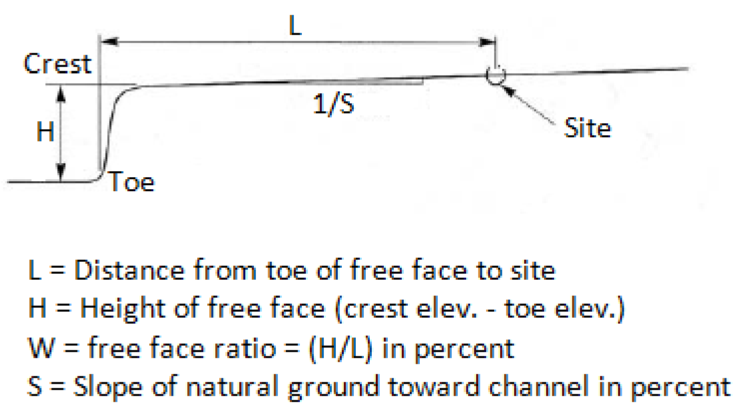

Figure 22. Slope geometry notation

Check the applicability of the Youd et al. (2002) model to the site of interest by comparing the parameters obtained in the preceding steps against the ranges shown in **Table 12**. The results of any analyses based on parameters that lie outside these ranges should be interpreted very carefully.

Table 12. Range of allowable variable values for use with the Youd et al. (2002) predictive equation

Variable	Description	Range
T_{15}	Equivalent thickness of saturated cohesionless soils (clay content ≤15%) in m.	1 to 15m
M	Moment magnitude of the earthquake	6.0 to 8.0
Z_T	Depth to the top of the shallowest layer contributing to T_{15}	1 to 15m
W	Free face ratio	1 to 20%
S	Ground slope	0.1 to 6%
F_{15}, $D50_{15}$	Applicable combinations of F_{15} and $D50_{15}$ should be obtained from the figure below	

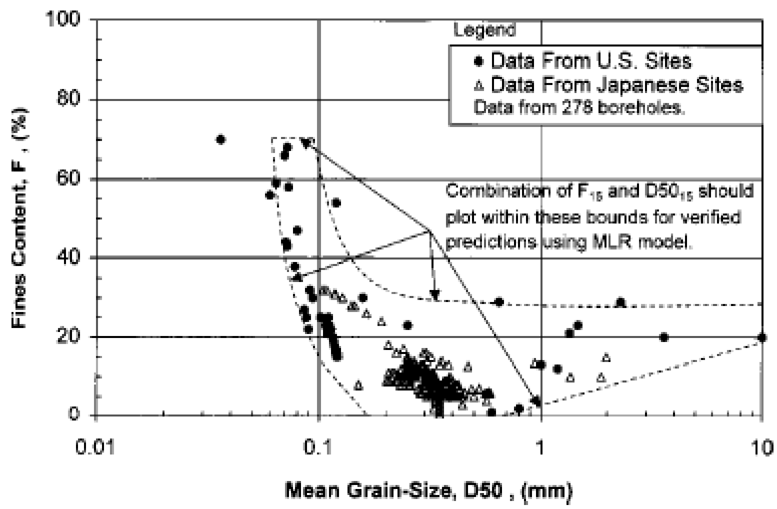

For given site conditions, the lateral spreading depends on the seismicity parameters M and D. Youd et al. (2002) provided the chart shown in **Figure 23** for obtaining the equivalent distance for use in **Equation 19**.

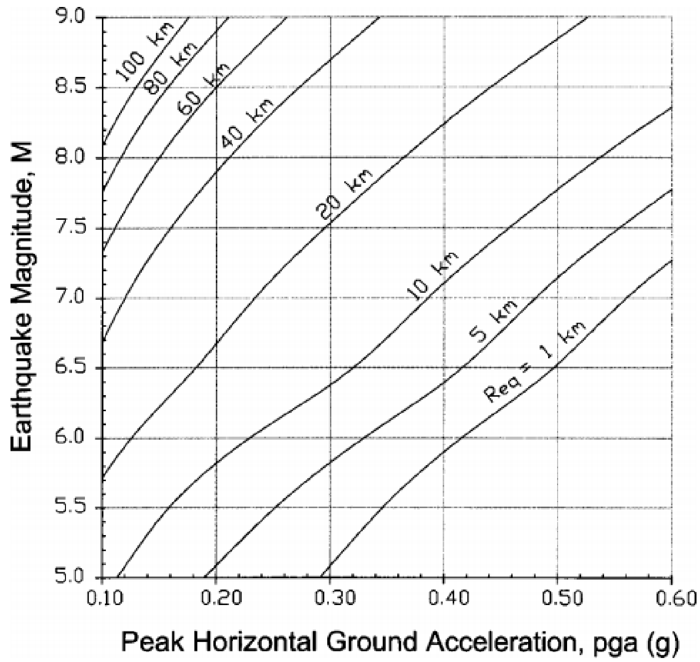

Figure 23. Graph for determining equivalent source distance, R_{eq}, for magnitude, M, and peak acceleration, a_{max}.

The above curves are the averages of PGA from three different attenuation relations: Abrahamson and Silva, 1997; Boore et al. 1997; and Campbell, 1997. For the Abrahamson and Silva, 1997 relation, the following parameters were used in the regression equation: R equals the distance to the fault rupture, fault type was set to ''otherwise'', HW5 hanging wall factor was set to 1, which implies that sites are found on the hanging wall, site classification was set to 1 for deep soil sites. For the Boore, Joyner and Fumal, 1997 relation, the following parameters were used in the regression equation: R is the closest horizontal distance in km to a vertical projection of fault rupture surface in km; V_s in the upper 30 of the site was set to 270m/s which is the mid - range for a medium stiff soil site, Class D, fault type was set to ''fault mechanism not specified.'' For the Campbell 1997 relation, the following parameters were used in the regression equation: R is the closest distance to the seismogenic rupture surface km, fault style factor was set to ''otherwise'', soft rock and hard rock site factors were set to ''otherwise'', which implies a stiff soil site.

4.3 Lateral Displacements using Magnitude-Distance Deaggregation

When dealing with probabilistic ground motions in BC, as pointed out in the Liquefaction Section, a magnitude M=7.0 is selected and paired with a peak probabilistic ground motion selected from either, a hazard analysis, or from a site response analysis using input motions which match the probabilistic design spectrum that has an exceedance rate of 2% in 50 years. This probabilistic acceleration is made up of the average site acceleration plus $\varepsilon\sigma$, where σ is the standard deviation and ε is the number of standard deviations required to reach the probabilistic value. For Vancouver the average ε=1.72. Using such a high acceleration in **Figure 23** results in overly short distances and consequently, inflated estimates of displacement.

Average acceleration method: The average acceleration at the site may be obtained by running a hazard analysis for the site with ε=0. An average acceleration of 0.20g for the Lower Mainland is appropriate. Using this average acceleration results in significantly longer distances, D, and correspondingly smaller lateral spreading displacements.

Deaggregation method: The deaggregation method used in evaluating liquefaction potential may also be used here. For each magnitude-distance pair in the deaggregation matrix, we compute the corresponding lateral displacements using Youd's **Equation (19)**. These displacements are then multiplied by the corresponding probability density given by the deaggregation for that magnitude-distance pair. This results in a new spreadsheet of lateral displacement values. The displacements corresponding to any magnitude bin are summed horizontally and then the sums at the end of each row are summed to give the total horizontal displacement.

The spreadsheet of displacements calculations used in the deaggregation method in shown in **Figure 24**. Cells that show zero values represent infinitely small displacements which are omitted for clarity. This spreadsheet also shows the clear separation of the contributions of the smaller and shallower earthquakes compared to the larger subcrustal earthquakes. Notice that influence of the latter kick in at distances of greater than 50km. The typical deaggregation available on the GSC Website (nrcan.gc.ca) is not suitable for this calculation because the distance bins are too large. If requesting a magnitude-distance deaggregation from GSC, specify a distance bin size of 5km.

	Distance Bins																
Magnitude Bins	2.5	7.5	12.5	17.5	22.5	27.5	32.5	37.5	42.5	47.5	52.5	57.5	62.5	67.5		197.5	Row Totals:
5.1	0	0	0	0	0	0	0	0	0	0	0	0	0	0		0	**0**
5.3	0	0	0	0	0	0	0	0	0	0	0	0	0	0		0	**0**
5.5	0	0.0001	0	0	0	0	0	0	0	0	0	0	0	0		0	**1E-04**
5.7	0	0.0004	0	0	0	0	0	0	0	0	0	0	0	0		0	**4E-04**
5.9	0	0.0008	0.0001	0	0	0	0	0	0	0	0	0	0	0		0	**9E-04**
6.1	0	0.0018	0.0003	0	0	0	0	0	0	0	0	0	0	0		0	**0.002**
6.3	0	0.0038	0.0007	0.0002	0	0	0	0	0	0	0.0001	0	0	0		0	**0.005**
6.5	0	0.0076	0.0017	0.0004	0.0001	0	0	0	0	0	0.0002	0.0002	0.0001	0		0	**0.01**
6.7	0	0.0145	0.0039	0.0011	0.0003	0.0001	0	0	0	0	0.0005	0.0004	0.0003	0.0002		0	**0.021**
6.9	0	0.0256	0.0082	0.0026	0.0009	0.0004	0.0001	0	0	0	0.0009	0.0008	0.0005	0.0004		0	**0.041**
7.1	0	0.0421	0.016	0.0057	0.0021	0.001	0.0004	0.0002	0.0001	0	0.0009	0.0008	0.0005	0.0004		0	**0.071**
7.3	0	0.064	0.0291	0.0119	0.0049	0.0024	0.001	0.0005	0.0003	0.0001	0	0	0	0		0	**0.114**
7.5	0	0.0897	0.0487	0.0227	0.0102	0.0053	0.0024	0.0014	0.0008	0.0004	0.0002	0.0001	0	0		0	**0.182**
7.7	0	0.0594	0.0374	0.0194	0.0095	0.0053	0.0026	0.0015	0.0009	0.0004	0.0003	0.0002	0	0		0	**0.137**
7.9	0	0	0	0	0	0	0	0	0	0	0	0	0	0	0	0	**0**
8.1	0	0	0	0	0	0	0	0	0	0	0	0	0	0	0	0	**0**
8.3	0	0	0	0	0	0	0	0	0	0	0	0	0	0	0	0	**0**
8.5	0	0	0	0	0	0	0	0	0	0	0	0	0	0	0		**0**
8.7	0	0	0	0	0	0	0	0	0	0	0	0	0	0	0		**0**
8.9	0	0	0	0	0	0	0	0	0	0	0	0	0	0	0		**0**
															Total of the Totals:		0.584

Figure 24. Sample calculation of lateral spreading displacements using the deaggregation method

Both of these methods are applied to a school project site in Delta to evaluate the lateral spreading displacements. The probabilistic PGA from site response analysis was 0.35g. The site parameters are as follows: average ground slope, S = 0.5%, $D50_{15}$ = 0.25mm, F_{15}=5% and T_{15} varies with location at the site. The T_{15} values for the 6 site locations are 8.60m, 8.80m, 7.75m, 9.95m, 4.95m and 7.95m, respectively. The lateral spreading displacements are calculated using Youd et al. (2001) following current practice. For M=7.0, a =0.35g, **Figure 23** gives an approximate distance R≈13km, Computed displacements using equation 2 are shown is green in **Figure 18**. The displacements are also calculated for M=7.0 and an average acceleration of 0.20g, which gives a distance R=25km, and are shown in blue in **Figure 25**. Finally, the deaggregation method is also used and the results are shown in red in **Figure 25.** It `is clear that using the probabilistic peak ground acceleration to determine the equivalent distance for use in the Youd equation gives inflated estimates for lateral spreading displacement. it seems acceptable to estimate displacements on the basis of M=7.0 and an average site acceleration of 0.2g.

As was seen from **Figure 25**, the displacements computed using the deaggregation method and the average acceleration method are approximately 50% of the Youd et al. (2001) displacements. The difference with the Youd displacements is accounted for by the fact that the probabilistic acceleration, rather than the average acceleration, was used to calculate the displacements. These differences in displacement have very serious consequences for the retrofit program. If refined magnitude=distance deaggregation is not available from GSC to allow effective use of the deaggregation method, it is recommended that future displacements for school projects be estimated using the Youd et al. procedure with an average acceleration of 0.20g and M=7.0.

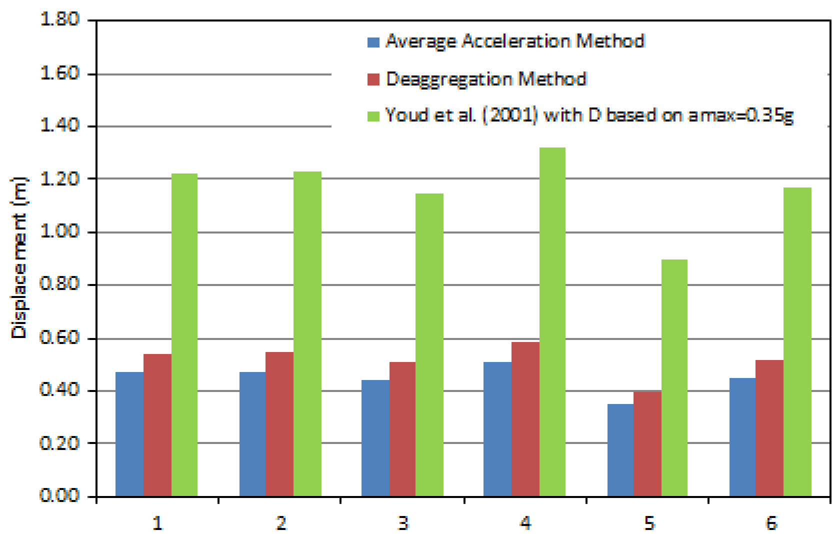

Figure 25. Calculated displacements for the school site in Delta

4.4 Idriss and Boulanger (2008) Model

Idriss and Boulanger (2008) and Zhang et al. (2004) present methods for estimating lateral spreading displacements based on laboratory test data. Idriss and Boulanger (2008) present a method for estimating the maximum shear strains that may occur in a liquefiable layer during earthquake shaking. Their procedure is based on shear strains estimated from cyclic laboratory testing of saturated sands at various densities by Ishihara & Yoshimine (1992). The maximum shear strains are limited to the bounds proposed by Seed et al. (1985) and shown in **Figure 26**, which were computed using **Equation (20)** (Idriss and Boulanger 2008).

$$\gamma_{lim} = 1.859\left(1.1-\sqrt{\frac{(N_1)_{60,cs}}{46}}\right)^3 \tag{20}$$

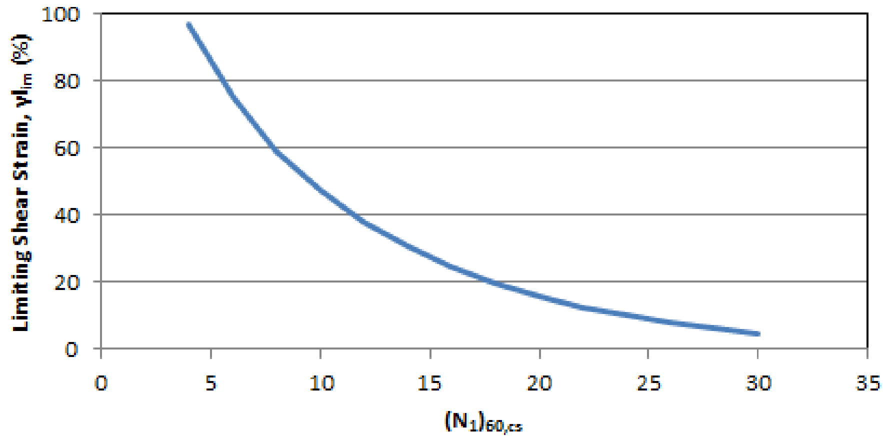

Figure 26. Limiting shear strains, γ_l, as a function of $(N_1)_{60,cs}$

The lateral displacement, LD, is computed using **Equation (21)**

$$LD = \int_0^{Z_{max}} \gamma \, dz \tag{21}$$

4.5 Zhang et al. (2004) Model

Zhang et al. (2004) made use of a laboratory test-based relationship among “maximum cyclic shear strain,” relative density, and factor of safety against liquefaction (Ishihara and Yoshimine, 1992) to develop a cumulative shear strain model for predicting maximum lateral spreading deformations using **Equation (22)**. He introduced the term Lateral Displacement Index (LDI) to describe these lateral displacements.

$$LDI = \int_0^{Z_{max}} \gamma_{max} dz \tag{22}$$

Maximum cyclic shear strains were defined by Ishihara and Yoshimine (1992) as the maximum shear strain (in any direction) under transient loading conditions. Zhang et al. (2004) capped the maximum cyclic shear strains by the limiting shear strains proposed by Seed (1979) and used empirical relationships between relative density and penetration resistance (SPT or CPT) to allow lateral spreading displacement to be predicted. Using the penetration resistance and factor of safety against liquefaction (**Figure 27)** to determine the maximum shear strain, γ_{max}. Zhang et al. (2004) recommend the use of a modified form of Meyerhof's relationship to estimate relative density as

$$D_r=16\sqrt{(N_1)_{78}}=14\sqrt{(N_1)_{60}} \text{ for } (N_1)_{60} < 42. \qquad \textbf{(23)}$$

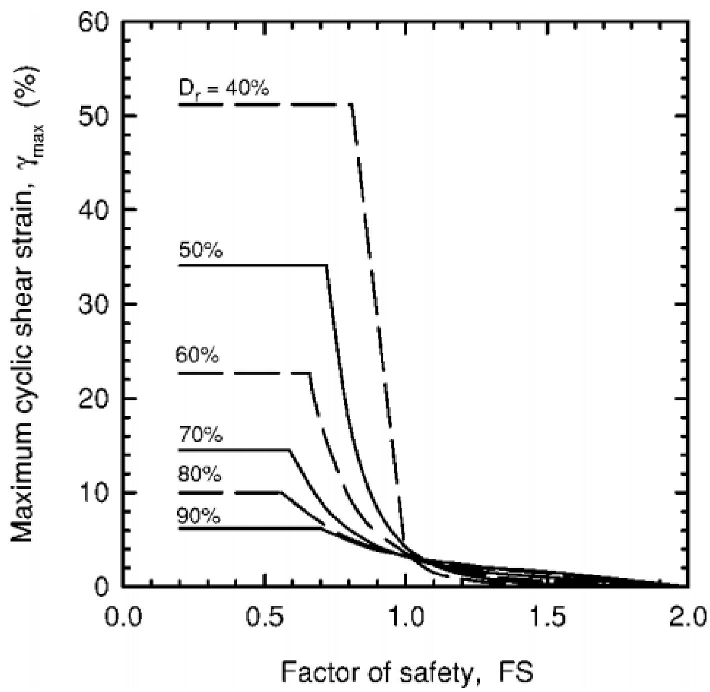

Figure 27. Variation of maximum cyclic shear strain with factor of safety and relative density (after Zhang et al., 2004)

Zhang et al. (2004) modified the LDI on the basis of field data of observed lateral displacements. The modified equations are given in **Equation (24)** for displacements due to sloping ground and a free face.

$$D_H=\begin{cases}(S+0.2)LDI, & \text{ground slope case}\\ 6W^{-0.8}LDI, & \text{free face case}\end{cases} \qquad \textbf{(24)}$$

The lateral displacements calculated by Youd et al. (2002), Idriss and Boulanger (2008) and Zhang et al. (2004) for a school site in Delta are shown in **Figure 28**. It is clear that Idriss and Boulanger (2008) seriously overestimate the displacements. This results from the fact that the displacement estimates are based entirely on shear strains without correlation with field data. As shown in **Figure 25**, displacements calculated by the average acceleration or the deaggregation method are approximately 50% of those calculated by Youd et al. (2001). These differences in displacement estimates can have a very significant impact on the potential performance of a school on this site. It is recommended that lateral spreading be estimated using both the average acceleration and the deaggregation methods.

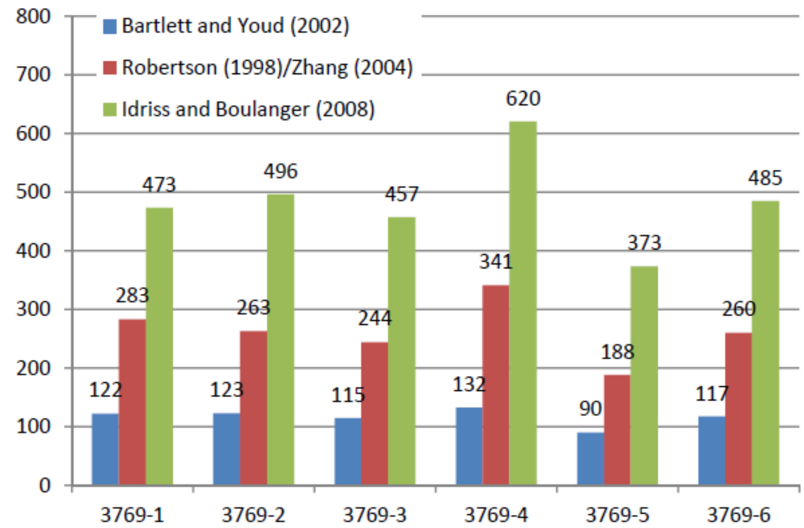

Figure 28. Lateral spreading displacements for school site in Delta using three different methods (Figure courtesy of John Carter, GeoPacific Ltd.)

4.6 Vertical Settlements due to Consolidation after Liquefaction

4.6.1 Ishihara & Yoshimine (1992) Model

The Ishihara & Yoshimine (1992) used the factor of safety against liquefaction, *FS*L, and various indicators of soil density (relative density, SPT resistance, and CPT resistance) to predict volumetric strain. The graphical relationship (**Figure 29**) shows that volumetric strains increase when the factor of safety drops below 1.0 – sharply for looser sands and gradually for denser ones. The Japanese SPT value, N_1, used in **Figure 29**, however, is based on an energy ratio of 72% (i.e., ($N_1 = 0.833(N_1)_{60}$).

The volumetric strain strains developed from **Figure 29** are based on the factor of safety against liquefaction. These factors should be based on either the deaggregation method described in the liquefaction section (preferred) or use the mean magnitude with the probabilistic ground motions otherwise the settlements will be overestimated.

Idriss and Boulanger (2008, pp152-158) present a very useful discussion on strain based methods for settlement calculations. Ishihara & Yoshimine (1992) procedure is recommended here for the present. More detailed study of settlement calculations will be conducted when the new motions for NBCC 2015 become available and will be reflected in the revised guidelines.

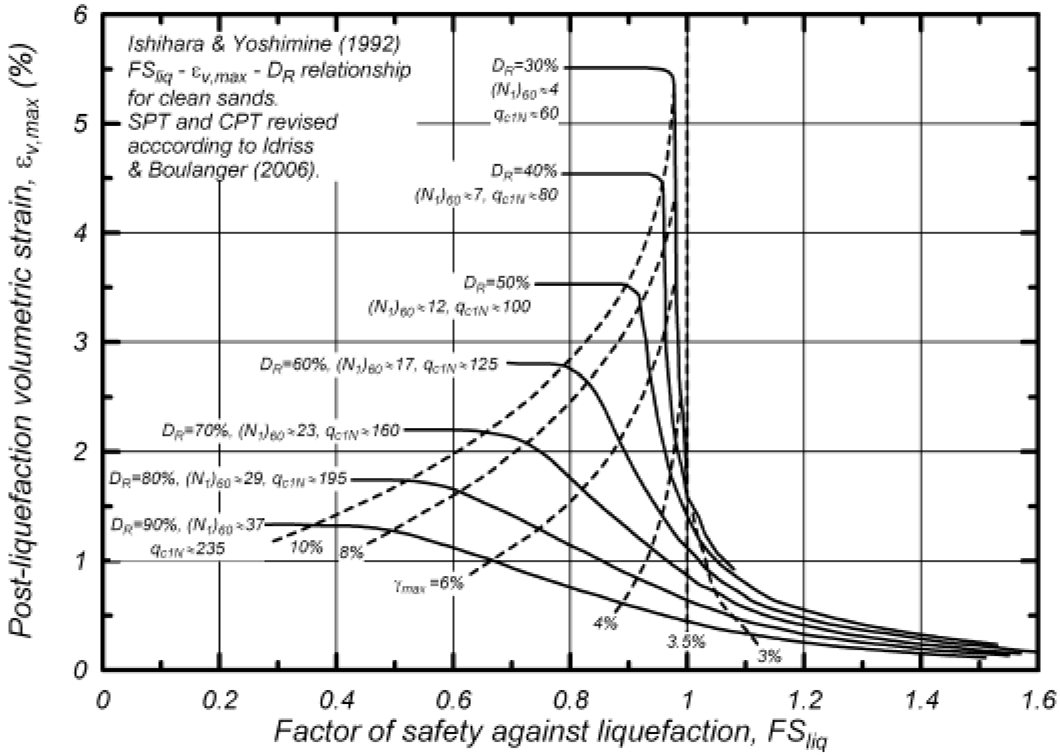

Figure 29. Variation of volumetric strain with relative density, SPT and CPT resistance, and factor of safety against liquefaction (after Ishihara & Yoshimine, 1992).

Using the curves in **Figure 29** and FSL and density parameters, determine the corresponding values of volumetric strain. The expected settlement, ΔH, is obtained as the sum of all sublayer settlements, which are approximated assuming constant volumetric strain within each sublayer.

$$\Delta H = \sum_{i=1}^{n} t_i \varepsilon_{v,i} \qquad \textbf{(25)}$$

where *n* is the number of sublayers and l_i is the thickness of the i^{th} layer.

5.0 Structural Considerations

5.1 General

The evaluation of the effects of liquefaction on a structure is based on the following, for the purposes of these Guidelines:

- During strong shaking, the soil has not liquefied and the demand is as for a Class D/E site with no degradation of the soil strength or stiffness; the typical assessment or retrofit design as outlined in the remainder of the Volumes applies. The block must be assessed or retrofitted as if liquefaction is not an issue.
- After strong shaking, on a liquefiable site, the soil liquefies and induces new and different demands on the structure. The block must be assessed or retrofitted to accommodate these demands, starting in a partially damaged state as per 5.2.4.
- The above two effects are not concurrent
- The structure must be assessed and retrofitted to accommodate both effects
- If the soil will be improved to eliminate the potential for liquefaction, then the demands have to be re-assessed for strong shaking effects only, based on the new site Class after the soil improvement

The structural assessment regarding liquefaction is outlined in this Section and retrofit considerations are outlined in Section 6 of this Volume.

Effective communication between the structural engineer and the geotechnical engineer is essential in the assessment of the demands of liquefaction and its influence on the structural response, and to obtain appropriate geotechnical parameters in order to carry out a retrofit design.

5.2 Assessment

5.2.1 Existing Information

The following information is essential in the assessment:

- Proper foundation drawings, and drawings of the ground floor slab
- Reasonable investigation to confirm the extent and depth of foundations as shown on the drawings (or to determine such information where adequate drawings do not exist)
- Determine the bearing pressure on all foundations, due to all self-weight (including additional dead loads as per NBCC 2010) and 25% of snow load plus 100% of storage loads and a Live Load allowance (LLa) of 1 kPa; C:DL+ADL+25%SL+100+ Storage+LLa.
- Adjacent blocks or structures and their surcharge loads on the foundation of the block being assessed; proximity effects for punching shear check.

- Fully understand the location of the LDRS, VLS, OP walls, and their drift limits.
- Knowledge of fundamental soil parameters such as, punching shear capacity of non-liquefiable soil layer, friction coefficient between soil and footings and between soil layers, passive pressures, modulus of subgrade reaction, down drag effects (if any) on piles, existing pile capacities, pile depths and expected behavior (friction or end bearing).

5.2.2 Foundations located in Non Liquefiable Crust

Most foundations will be located in a non-liquefiable crust, located over a liquefiable layer, as illustrated in (a), (b), (e) in **Figure 30** below (or located over a zone of a combination of liquefiable and non-liquefiable layers).

During liquefaction it is to be assumed that the liquefiable layer offers near-zero vertical resistance and the only soil resistance vertically is the soil between the underside of the foundation and the liquefiable layer.

The potential for punching shear failure of the foundations through the crust exists, and must be assessed.

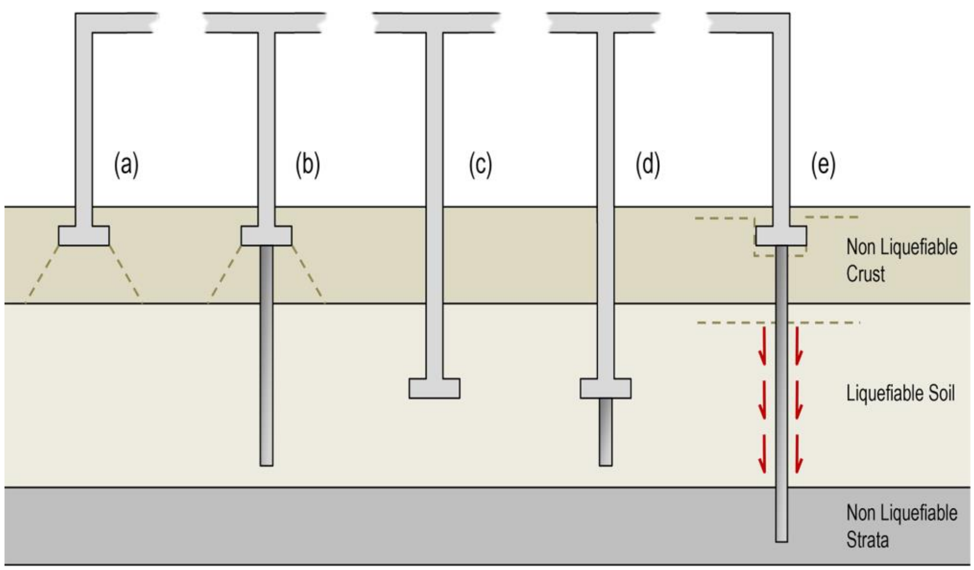

Figure 30. Foundations located in Crust or in Liquefiable Soil

The punching shear capacity of the soil (for individual pad footings or strip footings) as obtained from the geotechnical engineer shall be checked versus the calculated bearing pressure on the underside of the foundation for: all structural loads above grade, all structural related loads below grade, soil/slab above the footing outline.

a) Footing, no piles

b) Footing on piles that end within the liquefiable soil, assuming no vertical resistance from the piles; add weight of piles to structural loads to determine bearing pressure

In the case where the piles of a piled foundation extend through the liquefiable layer(s) to a firm non liquefiable strata, per (e) in the Figure above, the pile capacity shall be checked for the same loads as condition (a) above, plus the down drag on the pile (if any) of the liquefiable soil to be provided by the geotechnical engineer. Furthermore, the axial shortening of the pile and deflection of the pile tip in the lower strata shall be calculated by the geotechnical engineer and added to the differential vertical settlement discussed in **5.2.6** below, as applicable.

5.2.3 Foundations in liquefiable soil

Should the footings illustrated in condition (c) and (d) in the Figure above be fully founded in the liquefiable layer, no further assessment is required: remediation such as micropiles, soil densification, etc. is required.

5.2.4 Allowable structure drifts due to Liquefaction Effects

Due to the strong shaking prior to liquefaction, the residual drift in the structure (due to inelastic response, some damage) shall be assumed to be 20% of the DDL of the LDRS in each principal direction of the block (where the peak transient drift during strong shaking is 100% of the DDL).

The maximum allowable drift due to liquefaction effects shall be the Maximum DDL of the LDRS as outlined in Table 4.1, Part B, Volume 2, or the Design Drift Limit for VLS as outlined in Table 8.1, Part B, Volume 2, whichever is less.

With regards to the LDRS, the Maximum DDL is allowable, regardless of what DDL was used to accommodate the strong shaking effects.

Liquefaction Drift Limit (LDL) shall accommodate the following three components:

- Residual Drift (RD)
- Effective Drift demand due to lateral soil (horizontal) spreading effects (EDH)
- Effective Drift demand due to differential vertical soil settlement effects (EDV)

Thus RD + EDH + EDV < LDL

For example:

DDL	1% (less than Max DDL for reasons such as toolbox)
Residual Drift @ 20% of DDL	0.2%
Max DDL	2.25% (such as prototype M-3)
VLS limit	4% (such as steel)
LDL	2.25%, lesser of the two governs
EDH	1.5% (see 4.2.(5) below regarding how to determine EDH
EDV	0.8% (see 4.2.(6) below regarding how to determine EDV

Therefore, 0.2% + 1.5% + 0.8% = 2.5% which is greater than the 2.25% LDL; therefore remediation is required.

5.2.5 Lateral soil spreading effects

The lateral soil spreading effect, ΔH, due to liquefaction shall be determined on all sides of a block, as shown in **Figure 31** below.

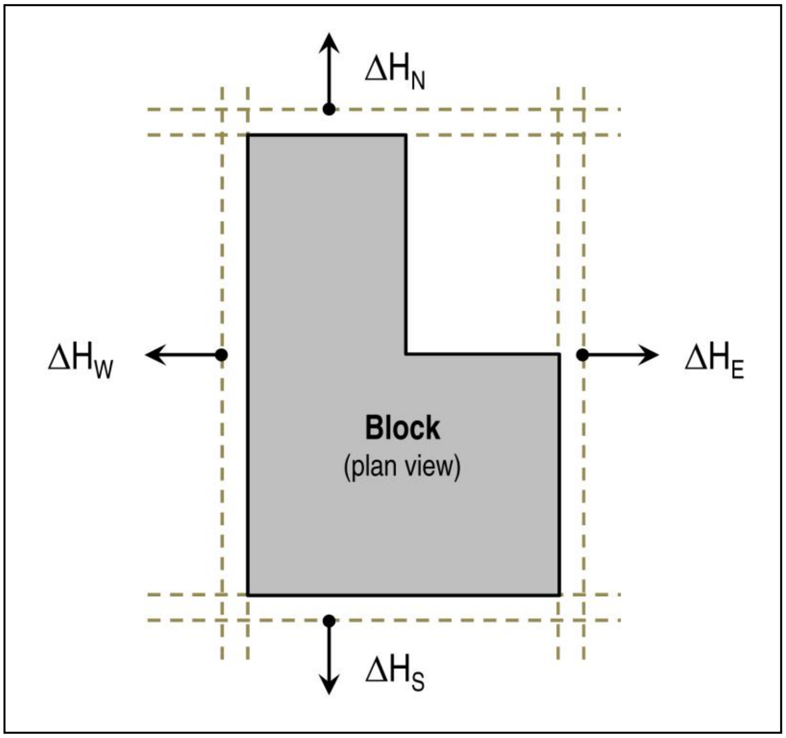

Figure 31. Lateral soil spreading effects on all sides of block

For the purposes of assessment, it is assumed that the crust can 'rupture' and cause a movement of ΔH between any non-interconnected foundations, or bay lines, or VLS or line of LDRS in the block and shall be provided by the geotechnical engineer. This "rupture" is illustrated in **Figure 32**; between two lines of footings on (a) and (b) in the section, and between any line of footings in the plan view.

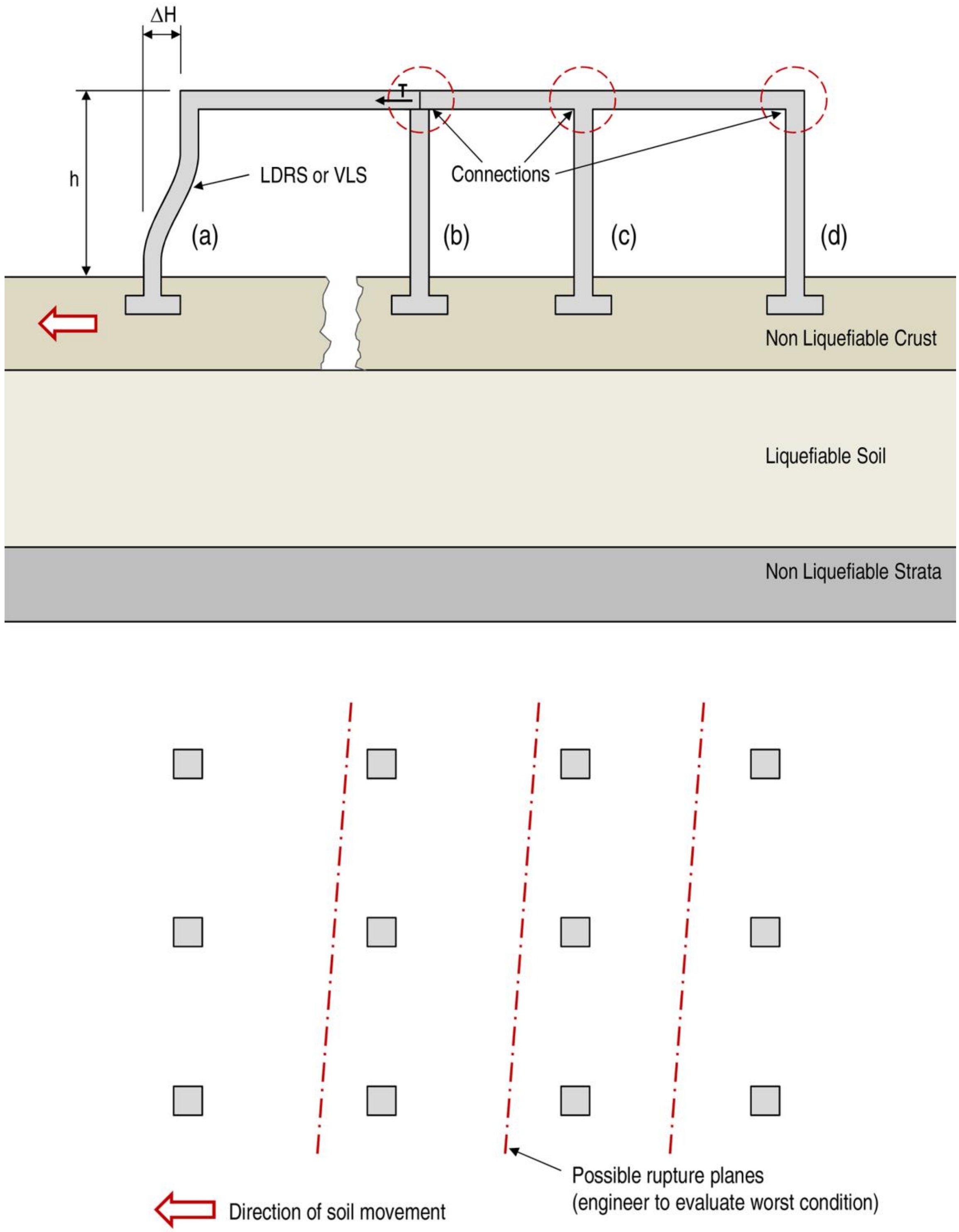

Figure 32. Lateral soil spreading effects

The resulting drift demand EDH is ΔH/h in percent; this is one of the three drift items noted in 4.2.4 above. This drift shall be calculated for each principal direction of the block, using the maximum ΔH provided by the geotechnical engineer in that direction.

If ΔH is unknown in one of the principal directions, 50% of the ΔH in the known direction shall be used for the orthogonal direction.

Further to the discussion above, alternative scenarios should be considered regarding where ΔH could occur at the foundation level, between non-interconnected footings or where weak interconnections exist, where such a movement could cause distress to VLS or floor/roof slabs due to such localized differential horizontal movements. This is illustrated in **Figure 33** below.

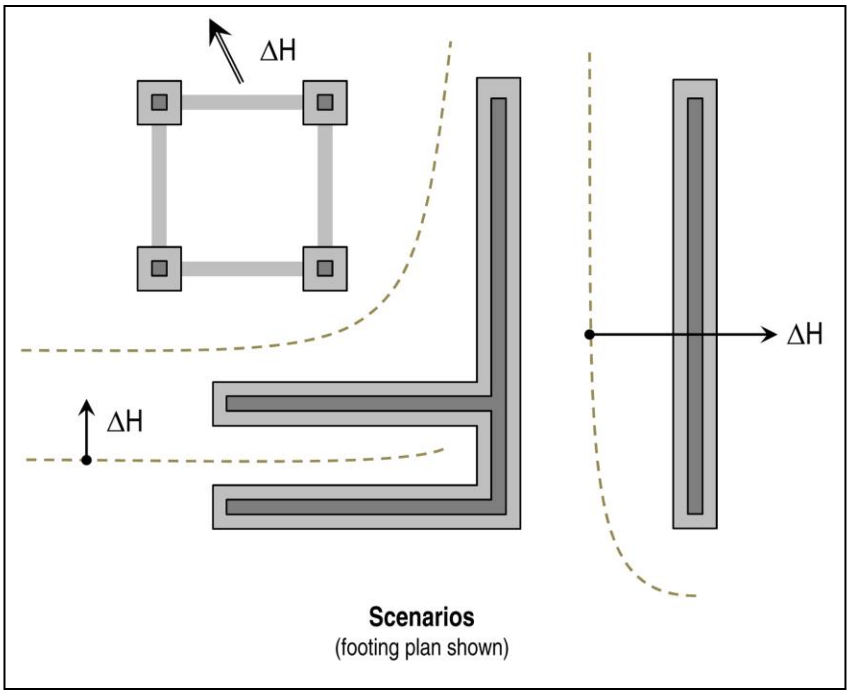

Figure 33. Possible alternate scenarios to consider

5.2.6 Differential vertical settlement effects

The differential vertical settlement due to liquefaction, ΔV, within the perimeter of a given block shall be determined by the geotechnical engineer; this shall be one value used for the entire block. This is illustrated as occurring between two adjacent non-interconnected foundations, in **Figure 34** below.

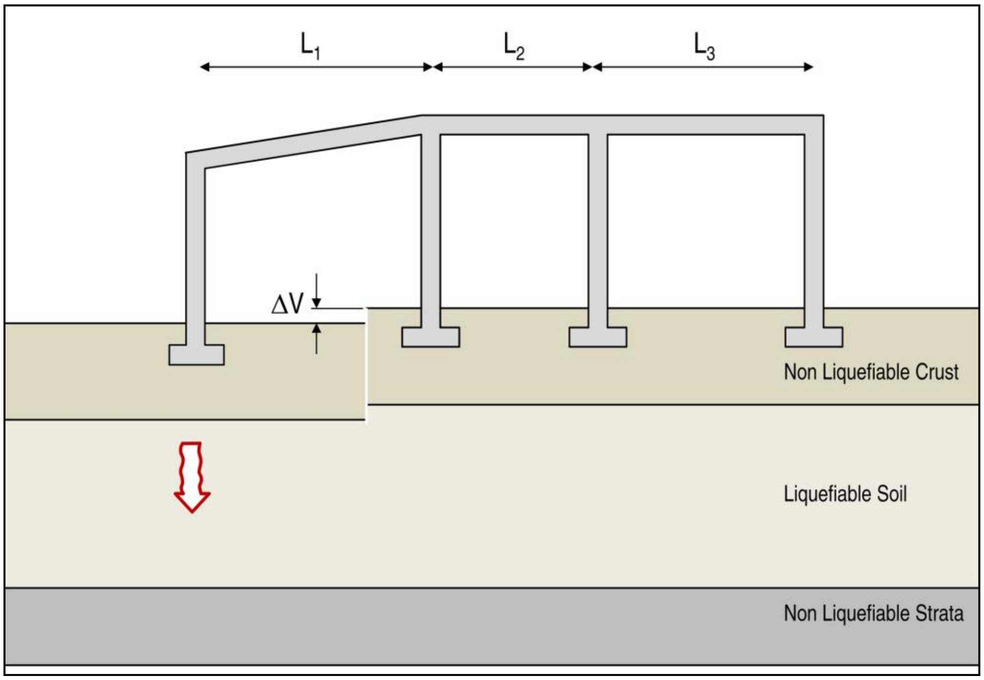

Figure 34. Differential Vertical Settlement Effects

For the purposes of assessment, it is assumed that the crust can 'shear' to accommodate the uneven settlements in the liquefiable soil layer and cause a movement of ΔV between any foundations non-interconnected or connected by an element without adequate capacity to accommodate the differential settlement, or baylines, or VLS or line of LDRS in the block.

The resulting effective drift demand EDV is $\Delta V/L1$ (as shown in **Figure 34**), or it can be $\Delta V/L2$ or $\Delta V/L3$ in the other spans shown, in percent. These effective drifts shall be calculated for each principal direction of the block, using the maximum effective drift demand in a given direction.

This calculated drift EDV is one of the three drift terms noted in 5.2.4.

5.2.7 Connections

Connections affected by rotation and/or lateral loads shall be checked to ensure the new demands on the connections cannot cause local or global collapse.

Figure 32 illustrates discrete or integral connections that shall be checked for:

Any additional tension loads induced in the diaphragm due the lateral spreading effects

Any potential movement of the diaphragm, should the tension load induce local connection failure, and allow movement of the diaphragm (and its beams) relative to the local support of the diaphragm

All affected connections shall be investigated.

6.0 Remedial Options

6.1 General

Any remedial work required is based on providing life safety and prevention of collapse, so that an affected facility can be safely evacuated in the event of a major earthquake. Structures may or may not be re-usable after the event.

The options for mitigation of liquefaction and its consequences for an existing building will generally fall into two categories: soil remediation, or structural modifications.

6.2 Soil Remediation

There are a wide variety of techniques for soil remediation that can be used to mitigate the effects of liquefaction or excessive cyclic softening, such as:

- in-situ densification using vibro-replacement or vibro-compaction or dynamic compaction,
- in-situ strength and stiffening using compaction grouting, jet grouting, deep soil mixing, shallow soil mixing.
- excavate and replace with compacted engineered fill.
- load transfer to non-liquefiable materials using piling.

All of these techniques are disruptive for an existing facility and usually quite expensive, so that preferred methods very often are structural, whereby a building is retrofit to provide it with the ability to withstand large deflections either laterally or vertically or both, to a sufficient degree that allows safe egress for its occupants.

One possible exception to the foregoing is in the case where there is a significant lateral spreading hazard to the building by virtue of an adverse ground slope or proximity to a river bank or similar free face towards which the lateral spreading will migrate. In such a case the amount of lateral spread movement can sometimes be limited by the installation of a so-called “seismic dike”. This is a zone of ground improvement of the liquefiable material of dimensions sufficient to provide resistance to lateral spreading and post-earthquake stability. This can be achieved with a variety of in-situ soil improvement techniques. See the Vancouver Task Force (2007) report for more discussion of methods and design philosophy and references thereto. Of course a retrofit using a perimeter seismic dike can only provide a level of protection against lateral displacements, and vertical post-earthquake settlements and/or punching failure of shallow foundations remain to be dealt with structurally.

Idriss and Boulanger (2008, pp 167-183) present a very useful review of mitigation measures. Experience with school projects with liquefaction problems suggests that the first attempt at mitigation should be structural. Geotechnical mitigation efforts are usually more expensive. In addition to the direct cost of geotechnical mitigation, the process often requires finding alternative accommodation for the students – a major expense.

6.3 Structural Remediation

There are a wide variety of techniques for structural remediation that can be used to mitigate the effects of liquefaction, if there are deficiencies in the structure and foundation based on the assessment in Section 4.

6.3.1 For inadequate punching shear capacity

(a) enlarging footings based on punching shear capacity provided by the geotechnical engineer

(b) adding mini-piles between existing footings, with a new grade beam connected to existing footing; the minipiles and the new grade beams to be designed to resist 100% of the loads unless it can be shown otherwise

(c) creating a complete raft foundation, interconnecting all existing footings; geotechnical engineer to provide modulus of subgrade reaction for raft footing design

6.3.2 For excessive lateral spread effects

(a) Interconnect all footings inside the building, with new tension ties.

(b) Create an external ring beam (fully or partially around perimeter as required) to minimize differential movement between footings.

The compression struts or slab on grade within the building perimeter to be designed to resist all sliding forces applied to them.

(c) Creating a complete raft foundation, interconnecting all existing footings.

(d) LDRS that has larger maximum DDL (to increase drift limit).

(e) Supplementary supports at adversely affected VLS (to increase drift limit).

(f) Modify VLS to accommodate larger drift limits; for example, if short columns created by partial height infills limit the DDL, add deflection gaps to eliminate the short column effect and increase the DDL of the system.

6.3.3 For excessive differential vertical settlements

Similar to 1 (b) noted above

Similar to 2 (c), (d) and (e) noted above

6.4 Enhanced Performance Retrofit

For blocks with an objective of Enhanced Performance Retrofit the concept of distortion damage should be considered and evaluated. The relationship between angular distortion ß and lateral strain ε_L to be kept below the “Severe to very severe damage” area as shown in **Figure 35** below.

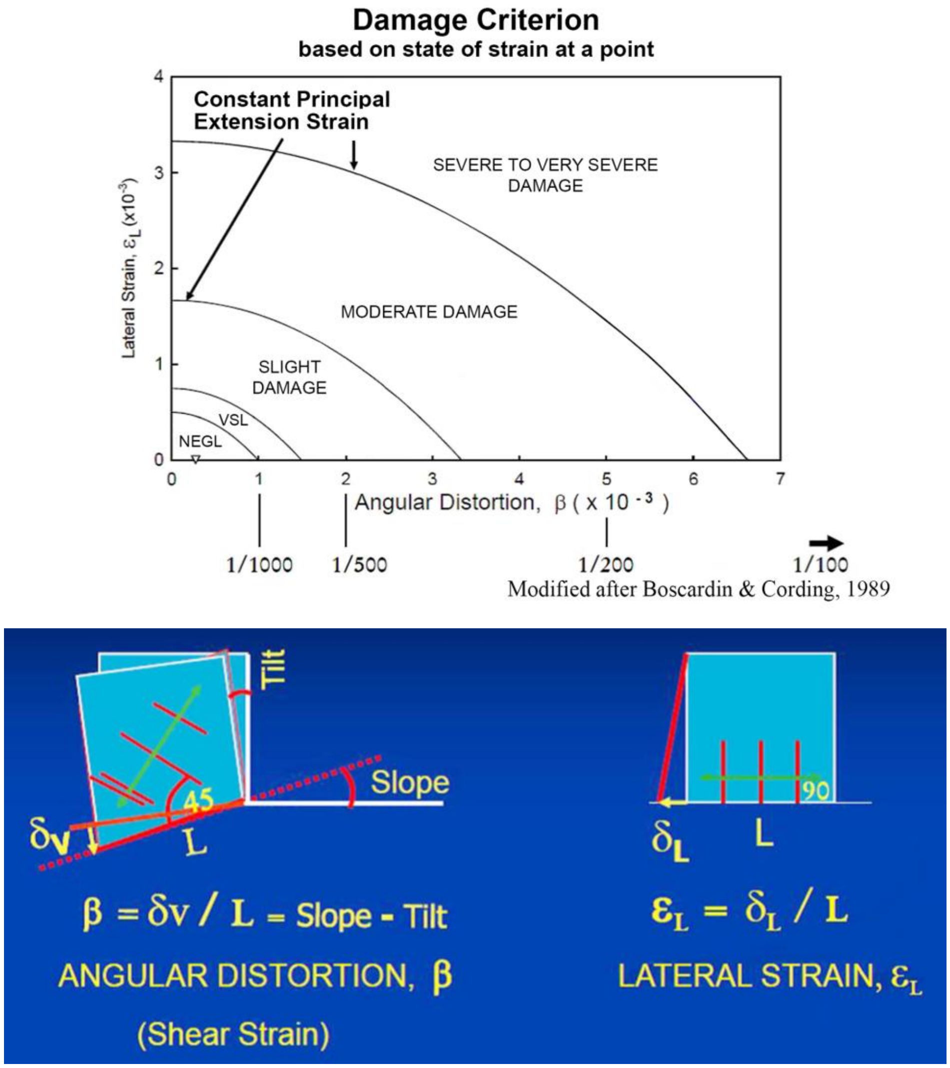

Figure 35. Damage Criteria consideration for Enhanced Performance Retrofit

For further information, refer to Boscardin and Cording (1989).

7.0 Closing the Loop: Reconciling Geotechnical Demands with Performance Criteria

The following example comes from a seismic retrofit study for a school in Vancouver. Atypical block is shown in **Figure 36**. The structural engineer responsible for the retrofit is John Sherstobitoff, Ausenco Ltd., Vancouver. The performance criteria set out in **Section 7.1** are taken from the **Seismic Retrofit Design Guidelines for Schools, 2nd Edition, 2013.**

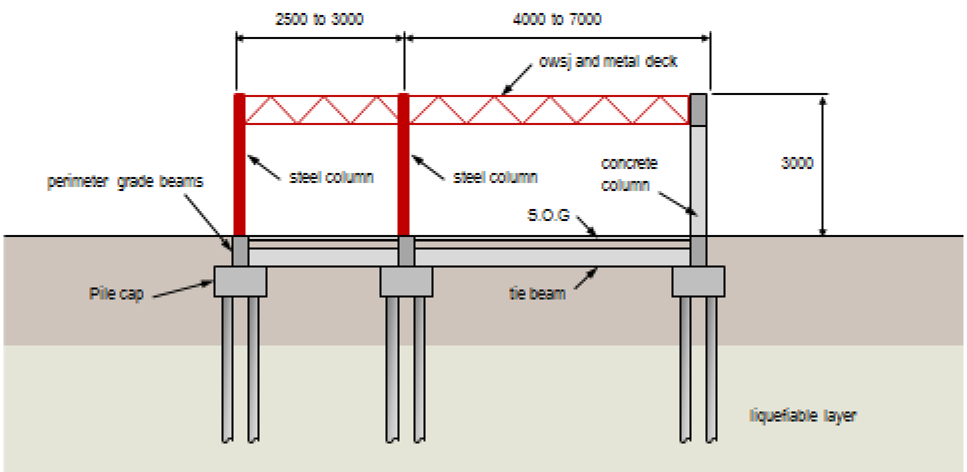

Figure 36. Cross-section of school building block

7.1 Performance Limits for School

Building Description

- One storey mixed concrete and steel framed structure
- LDRS Concentric braced frame
  (Tension-Compression moderately ductile)
  - **DDL: 2.5%**
- VLS Exterior: Non-ductile concrete columns
  - **DDL: 1.25%**
- VLS Interior/Exterior: Steel columns
  - **DDL: 4%**
- Liquefaction Drift Limit
  - **LDL: 4% or 2.5% * lesser of the two**
  - *** if liquefaction effects can cause such deformation**

7.2 Estimation of Total Drift

Drift Components to be considered are

- Residual drift (RD) from seismic excitation
- Effective drift demand due to lateral soil spreading (EDH)
- Effective drift demand due to vertical soil settlement (EDV)
- RD + EDH + EDV < LDL

These are illustrated in **Figure 37.** EDV is not a drift. A pseudo drift is computed using the settlement Δ V. This is added to the other drifts to give a conservative estimate of total drift demand.

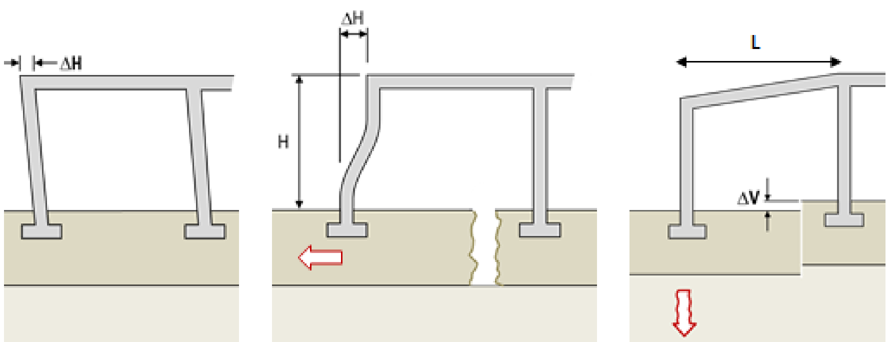

Figure 37. Summing up the displacement from different sources

7.3 Geotechnical Engineer Input

Geotechnical Engineer to provide

- Differential free field vertical movement
- Differential free field horizontal movement
- Friction coefficient between soil and foundations
- Bearing capacity on crust
- Soil pressure on grade beams
- Based on vertical loads at each foundation provided by the Structural Engineer, the Geotechnical Engineer will determine if there is risk of punching for each foundation
- Differential movement is too large, since the existing foundations are not adequately tied together in two directions

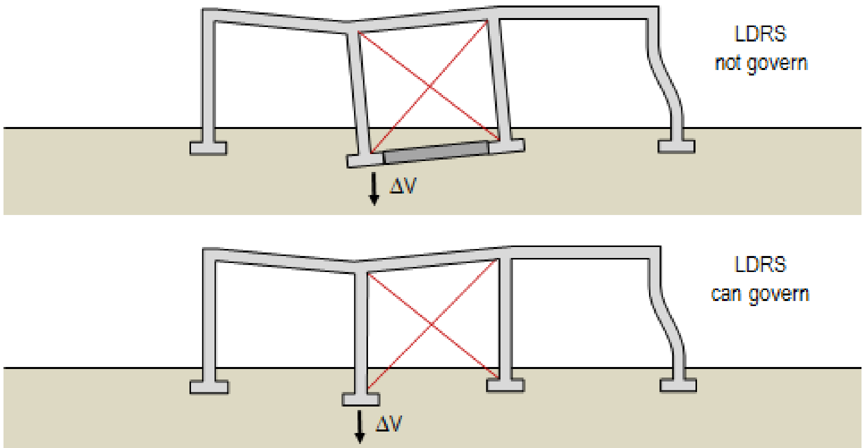

Figure 38. Effect of tying foundations together with grade beams.

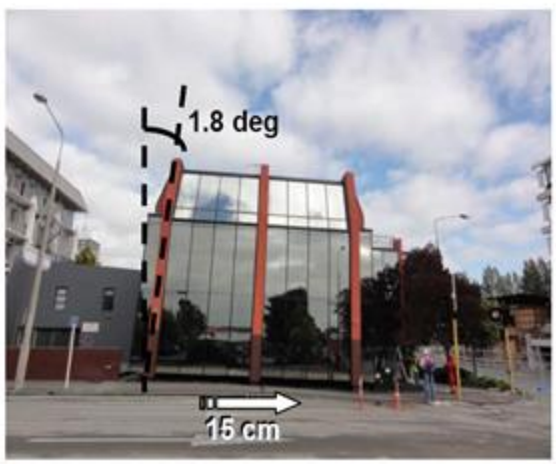

Figure 39. Building in Christchurch underwent rotation but no relative displacement across the base during the Canterbury earthquake.

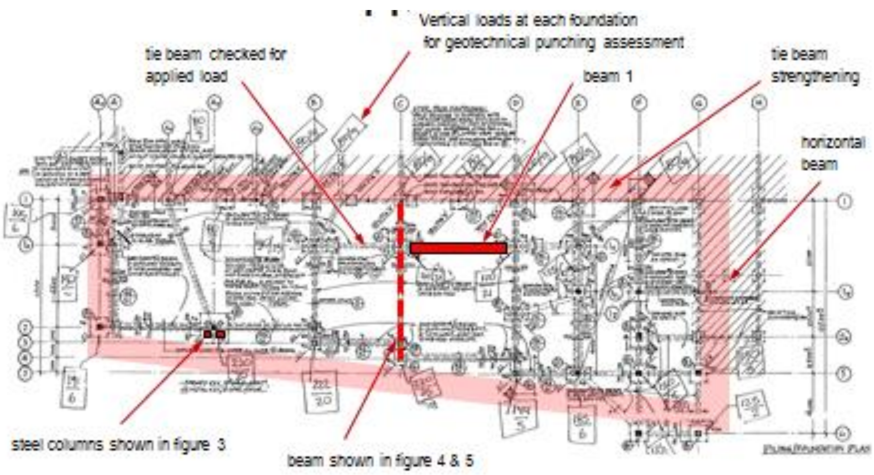

Figure 40. Plan of Building

7.4 Retrofit Details

Total drift due to liquefaction: 3.86 %. The designer decided to add two exterior steel columns at each side of the existing concrete columns to minimize the impact to the inside of the building, The new steel columns were designed to carry all the loads carried by the existing concrete columns. This retrofit option allowed an increase in the DDL of the VLS to 4% which can accommodate the liquefaction driven drift of 3.86% to be accommodated.

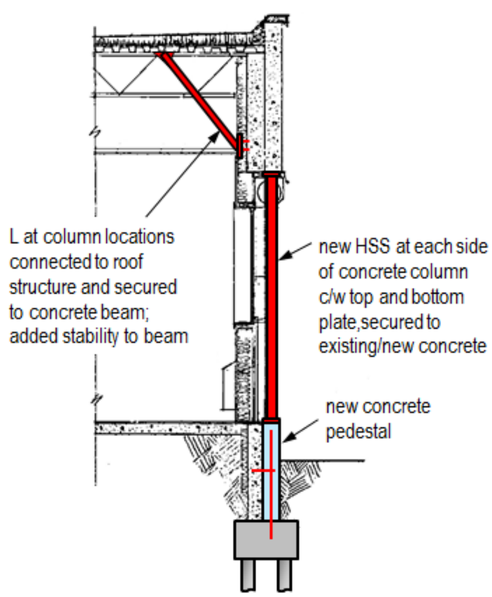

Figure 41. Plan of Building

7.5 Finished Project

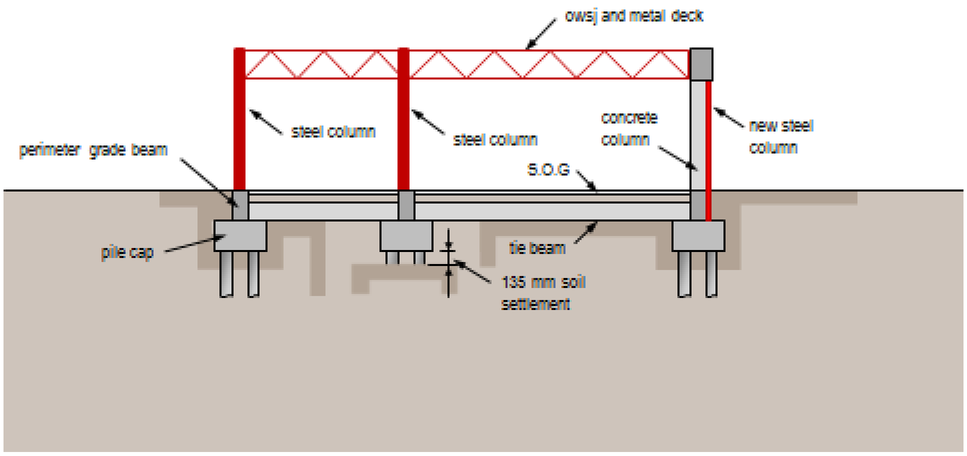

Figure 42. Finished Project

8.0 References

Andrus, R.D., Stokoe, K.H., Chung, R.M., and Juang, C.H. (2003). *Guidelines for Evaluating Liquefaction Resistance Using Shear Wave Velocity Measurements and Simplified Procedures*. NIST GCR 03-854, National Institute of Standards and Technology, Gaithersburg, MD, USA.

Andrus, R.D. and Youd, T.L. (1987). *Subsurface Investigation of a Liquefaction-Induced Lateral Spread, Thousand Springs Valley, Idaho*. US Army Corps of Engineers, Miscellaneous Paper GL-87-88.

Andrus, R.D. and Stokoe, K.H. (2000). Liquefaction resistance of soils from shear-wave velocity. *ASCE Journal of Geotechnical and Geoenvironmental Engineering*, **126**(11): 1015-1025.

Bartlett, S.F. and Youd, T.L. (1995). Empirical prediction of liquefaction-induced lateral spread. *ASCE Journal of Geotechnical Engineering*, **121**(4): 316-329.

Bjerrum, L. (1972). Embankments on soft ground. In: *Proceedings of the ASCE Conference on Performance of Earth-Supported Structures*, Purdue University, 2, 1-54.

Boscardin, M.D. and Cording, E.J. (1989). Building Response to Excavation-Induced Settlement. *ASCE Journal of Geotechnical Engineering*, **115**(1): 1-21.

Boulanger, R.W. and Idriss, I.M. (2004). *Evaluating the Potential for Liquefaction or Cyclic Failure of Silts and Clays, Report No. UCD/CGM-04/01*, Center for Geotechnical Modeling, Department of Civil and Environmental Engineering, University of California, Davis, USA.

Boulanger, R.W. and Idriss, I.M. (2014). Reply to discussion of CPT-Based Liquefaction Triggering Procedure. To appear in *ASCE Journal of Geotechnical and Geoenvironmental Engineering*, 2014.

Cetin, K., Seed, R., Der Kiureghian, A., Tokimatsu, K., Harder, L., Jr., Kayen, R., and Moss, R. (2004). Standard Penetration Test-Based Probabilistic and Deterministic Assessment of Seismic Soil Liquefaction Potential. *ASCE Journal of Geotechnical and Geoenvironmental Engineering*, **130**(12): 1314-1340.

DeGroot, D.J. and Ladd, C.C. (2012). Site Characterization for Cohesive Soil Deposits Using Combined In Situ and Laboratory Testing. Geo-Congress 2012 SOP Lecture, *ASCE Geotechnical Special Publication No. 226*.

Dobry, R. and Abdoun, T. (2011). *An investigation into why liquefaction charts work: A necessary step towards integrating the states of art and practice*. Ishihara Lecture, 5th International Conference on Earthquake Geotechnical Engineering, Santiago, Chile.

Finn, W.D.L. and Wightman, A. (2007). Logical Evaluation of Liquefaction Potential using NBCC 2005 Probabilistic Accelerations. In: *Proceedings, Ninth Canadian Conference on Earthquake Engineering*, Ottawa, Ontario, Canada, 1894-1993.

Halchuk, S. and Adams, J. (2006). *Updated deaggregation of seismic hazard for selected Canadian cities*, Personal communication to the authors in advance of publication, Geological Survey of Canada, Ottawa, Canada.

Idriss, I.M. (1985). Evaluating seismic risk in engineering practice. *In: Proceedings of the 11th International Conference on Soil Mechanics and Foundation Engineering*, Vol 1, 255-320.

Idriss, I.M. (1990). Response of soft soil sites during earthquakes. *In: Duncan, M. (Ed.) Proceedings H.B. Seed Memorial Symposium*, BiTech Publishers Ltd., Vancouver, BC, Canada. Vol.2, 273-290.

Idriss, I.M. and Boulanger, R. (2008). *Soil liquefaction during earthquakes*. MNO-12, Earthquake Engineering Research Institute, Oakland, California.

Ishihara, K. and Yoshimine, M. (1992). Evaluation of settlements in sand deposits following liquefaction During earthquakes. *Soils and Foundations*, **32**(1): 173-188.

Ladd, C.C., Foott, R., Ishihara, K., Schlosser, F., and Poulos, H. G. (1977). Stress-deformation and strength characteristics: SOA Report, *In: Proceedings, 9th International Conference on Soil Mechanics and Foundation Engineering*, Vol. 2, 421–494.

Ladd, C.C. and DeGroot, D.J. (2003). Recommended practice for soft ground site characterization: Arthur Casagrande Lecture. In: Culligan, P.J., Einstein, H.H. and Whittle, A.J. (Eds.). *Proceedings Soil and Rock America, Vol. 1*, Verlag Gluckauf GMBH, Essen, Germany.

Robertson, P.K. and Cabal (Robertson), K.L. (2010). *Guide to Cone Penetration Testing for Geotechnical Engineering, 4th Edition*. Gregg Drilling and Testing Incorporated, Signal Hill, California, USA.

SCEC, (1999). *Recommended procedures for implementation of DMG special publication 117, Guidelines for analyzing and mitigating liquefaction hazards in California, SCEC contribution number 462*, Southern California Earthquake Center, University of southern California, CA, 1-63.

Seed, H.B. and Idriss, I.M. (1971). Simplified Procedure for Evaluating Soil Liquefaction Potential, *ASCE Journal of Soil Mechanics and Foundations*, **97**(SM9): 1249–1273.

Seed, H.B. (1979). Soil liquefaction and cyclic mobility evaluation for level ground during earthquakes. *ASCE Journal of Geotechnical Engineering*, **105**(GT2): 201-255.

Seed, H.B., Tokimatsu, K., Harder, L.F. Jr. and Chung, R. (1985). Influence of SPT procedures in soil liquefaction resistance evaluations, *ASCE Journal of Geotechnical Engineering*, **111**(12): 1425-1445.

Vallee, R.P. and Skyrness, R.S. (1980). Sampling and In-Situ Density of a Saturated Gravel Deposit. *Geotechnical Testing Journal*, **2**(3): 136-142.

Task Force Report (2007). *Geotechnical Design Guidelines for Buildings on Liquefiable Sites in Accordance with NBC 2005 for Greater Vancouver Region*. Anderson, D.L. and Byrne, P.M. Co-Chairs.

Youd, T., Idriss, I., Andrus, R., Arango, I., Castro, G., Christian, J., Dobry, R., Finn, W.D.L., Harder, L., Jr., Hynes, M., Ishihara, K., Koester, J., Liao, S., Marcuson, W., III, Martin, G., Mitchell, J., Moriwaki, Y., Power, M., Robertson, P., Seed, R., and Stokoe, K.H. (2001). Liquefaction Resistance of Soils: Summary Report from the 1996 NCEER and 1998 NCEER/NSF Workshops on Evaluation of Liquefaction Resistance of Soils. *ASCE Journal of Geotechnical and Geoenvironmental Engineering*, **127**(10): 817–833.

Youd, T.L., Hansen, C.M. and Bartlett, S.F. (2002). Revised multilinear regression equations for prediction of lateral spread displacement. *ASCE Journal of Geotechnical and Geoenvironmental Engineering*, **128**(12): 1007-1017.

Zhang, G., Robertson, P.K. and Brachman, R.W.I. (2004). Estimating liquefaction-induced lateral displacements using the standard penetration test or cone penetration test. *ASCE Journal of Geotechnical and Geoenvironmental Engineering*, **130**(8): 861-871.